

**RAI Volume 3, Chapter 2.2.1.3.5, First Set, Number 2:**

Tabulate data summarized in the four uncertainty maps of net infiltration (SNL, 2008) for each of the four climate states. The information should include net infiltration and spatial coordinates. This information is needed to evaluate compliance with 10 CFR 63.114(a)(2).

**1. RESPONSE**

As discussed in the May 26, 2009, clarification call with the NRC, in addition to providing the tabulated data requested in the RAI, a discussion of the methodology for developing the infiltration maps, including the selection and scaling processes used, is provided. This response provides (1) preliminary pre-10,000-year period net infiltration output data for the four uncertainty scenarios for the three climate states used in downstream models (namely, *UZ Flow Models and Submodels* (SNL 2007a) and *Calibrated Unsaturated Zone Properties* (SNL 2007b)) and (2) a list of net infiltration maps used for the post-10,000-year period. For the pre-10,000-year period, the response summarizes the selection method of the net infiltration maps corresponding to the four uncertainty scenarios. For the post-10,000-year period, net infiltration was derived from the log-uniform (13 to 64 mm/yr) distribution of deep percolation flux ranges specified in the proposed 10 CFR 63.342(c)(2).

Development of net infiltration values for the pre-10,000-year period is summarized in Section 1.1. For the post-10,000-year period, a different approach was used. The net infiltration values were derived to be consistent with the average percolation flux range through the repository footprint specified in the NRC proposed 10 CFR 63.342(c)(2). DOE performed a detailed comparison between the proposed 10 CFR Part 63 and the final 10 CFR Part 63 that became effective on April 13, 2009 (see response to RAI 3.2.2.1.2.1-5-001).

Net infiltration data sources used in the unsaturated zone flow model are documented in *UZ Flow Models and Submodels* (SNL 2007a, Table 6.2-6).

**1.1 PRE-10,000-YEAR NET INFILTRATION CALCULATIONS**

For each of the three future climates (i.e., present-day, monsoon, and glacial-transition) spanning the 10,000-year period, two Latin Hypercube Sample (LHS) replicates of net infiltration input data were generated. Each replicate consisted of 20 realizations of input parameter values, totaling 40 realizations per climate state. Each realization produced a different map of spatially-varying infiltration across the infiltration model domain. From the 40 maps prepared for each climate state, four maps were selected to represent the uncertainty in each of the climate states (SNL 2008, Section 6.5.7). To identify the four uncertainty maps of net infiltration, the mean weighted net infiltration over the entire infiltration model domain was calculated for each of the 40 realizations. For each climate state, the distribution of mean weighted net infiltration values was used to select the 10th, 30th, 50th and 90th percentile values. These four values were used to identify the maps that most closely matched the 10th, 30th, 50th, and 90th percentiles of the probability distribution. The selected replicates and realizations are shown in Table 1.

Net infiltration values for the three pre-10,000-year climate states corresponding to the selected replicates and realizations are provided in the electronic files included with this response. These files contain net infiltration data with spatial coordinates. The spatial coordinates correspond to Easting and Northing coordinates of each grid cell in Universal Transverse Mercator (UTM) NAD 27, Zone 11 (meters) (SNL 2008). File names are given in Table 1 and also in Section 5, where the files are mapped to the corresponding enclosure numbers.

For the pre-10,000-year period, the net infiltration data originated in two cycles. Initial preliminary net infiltration values used in downstream models were obtained from calculations from the Mass Accounting System for Soil Infiltration and Flow (MASSIF) infiltration model described in *Simulation of Net Infiltration for Present-Day and Potential Future Climates* (SNL 2008, Appendix L). Although the preliminary net infiltration data were subsequently replaced by the final product outputs (SNL 2008, Section 8[a]), the preliminary net infiltration values were qualified for use in downstream models based on additional analysis against the final values. This additional analysis considered a number of comparisons between the preliminary and final data, and evaluated the potential impacts on downstream models due to data differences. It was found that the differences were small relative to the uncertainty and not statistically significant so that there was no impact from using the preliminary set of output.

For the additional analysis, the present-day, monsoon and glacial-transition mean infiltration values were calculated for the infiltration modeling domain, unsaturated zone modeling domain, and repository footprint for the 10th, 30th, 50th, and 90th percentile maps. For the present-day, 10th percentile infiltration map, the mean infiltration over the repository footprint changed from 4.03 mm/yr (preliminary data) to 3.87 mm/yr (final data). Infiltration values decreased in most cases. The largest increase in mean infiltration over the repository footprint was for the monsoon climate map, 50th percentile, increasing from 19.43 to 28.81 mm/yr. Increased mean infiltration over the repository footprint increased for the following cases: present-day climate, 90th percentile map; monsoon climate, 30th and 50th percentile maps, and glacial-transition climate, 50th percentile map. In the total system performance assessment (TSPA) probability weighting factors of 62%, 16%, 16%, and 6% derived from the generalized likelihood uncertainty evaluation (GLUE) procedure are applied to the 10th, 30th, 50th, and 90th percentile maps, respectively. The analysis indicated these changes are insignificant.

The following conclusions were made based on the analysis:

- Differences in the infiltration rates obtained for the different climate conditions using the preliminary and final infiltration data are not statistically significant
- Differences between the mean infiltration rates over the repository footprint, based on preliminary and final infiltration data, are not statistically significant
- Differences between the preliminary and final mean infiltration rates are small compared to the uncertainty in infiltration rates.

## 1.2 POST-10,000-YEAR NET INFILTRATION CALCULATIONS

The post-10,000-year period net infiltration maps were derived using the average percolation flux ranges specified in the proposed 10 CFR 63.342(c)(2) (SAR Section 2.3.2.4.1.2.4.2). The post-10,000-year percolation results were based on the proposed rule log-uniform (13 to 64 mm/yr) distribution (SNL 2007a, Section 6.1.4) and not the truncated log-normal (10 to 100 mm/yr) distribution as revised in the final rule. The percolation fluxes specified in the proposed rule were taken to be equal to the average net infiltration at ground surface through the projection of the repository footprint based on unsaturated zone flow model results (SNL 2007a, Section 6.1.4). Applying unsaturated zone flow calibration process results to the 10th, 30th, 50th, and 90th percentile uncertainty maps for the three pre-10,000-year climate states resulted in adjusted uncertainty weights using the GLUE procedure for those maps of 62%, 16%, 16%, and 6%, respectively (SNL 2007a, Table 6.8-1). The midpoints of the cumulative distributions of the adjusted uncertainty ranges are 31%, 70%, 86%, and 97%. Applying these adjusted, cumulative probability values to the log-uniform percolation flux distribution specified in the NRC-proposed 10 CFR 63.342(c)(2) provides four target net infiltration rates averaged over the repository footprint: 21.29, 39.52, 51.05, and 61.03 mm/yr (SNL 2007a, Table 6.1-3).

The 12 infiltration maps generated for the present-day, monsoon, and glacial-transition climate states in the pre-10,000-year period are the bases for the spatial variability of net infiltration for the post-10,000-year period (SNL 2007a, Section 6.1.4). The average infiltration values through the projected repository footprint for each of the 12 infiltration maps are shown in Table 2. Four infiltration maps with suitable average infiltration rates were then selected as follows. The description below details what was actually done for TSPA and is slightly different from that described in SNL (2007a, Section 6.1.4). This difference would result in different infiltration maps, but in either event, the average net infiltration rate over the repository footprint (Table 2), would satisfy 10 CFR 63.342(c)(2).

The pre-10,000-year maps were selected as follows:

- The map with the highest average infiltration rate through the repository footprint was selected for developing the post-10,000-year 90th percentile uncertainty map.
- The map with the second highest average infiltration rate through the repository footprint was selected for developing the post-10,000-year 50th percentile map.
- The map with the third highest average infiltration rate through the repository footprint was selected for developing the post-10,000-year 30th percentile map.
- The map with the fourth highest average infiltration rate through the repository footprint was selected for developing the post-10,000-year 10th percentile map.

The four selected net infiltration maps were then scaled so the average infiltration through the projected repository footprint would closely match the target values. The selected maps are identified and the scaling factors are provided in Table 3.

Table 1. Net Infiltration Scenario Selected Replicates and Realizations

Scenario (Percentile)	Replicate Number	Realization Number	File Name
<b>Present-Day Climate State</b>			
10th	2	18	<i>PD_R2_V18_Infiltration.txt</i>
30th	1	13	<i>PD_R1_V13_Infiltration.txt</i>
50th	1	18	<i>PD_R1_V18_Infiltration.txt</i>
90th	2	17	<i>PD_R2_V17_Infiltration.txt</i>
<b>Monsoon Climate State</b>			
10th	1	19	<i>MO_R1_V19_Infiltration.txt</i>
30th	1	17	<i>MO_R1_V17_Infiltration.txt</i>
50th	1	6	<i>MO_R1_V06_Infiltration.txt</i>
90th	2	15	<i>MO_R2_V15_Infiltration.txt</i>
<b>Glacial-Transition Climate State</b>			
10th	1	1	<i>GT_R1_V01_Infiltration.txt</i>
30th	1	2	<i>GT_R1_V02_Infiltration.txt</i>
50th	2	16	<i>GT_R2_V16_Infiltration.txt</i>
90th	1	5	<i>GT_R1_V05_Infiltration.txt</i>

Table 2. Calculated Average Net Infiltration Rate over the Repository Footprint for the Pre-10,000-Year Period

Net Infiltration Map Scenario (Percentile)	Unsaturated Zone Flow Model Upper Boundary Average Net Infiltration Rate over Repository Footprint (mm/yr)
Present-Day 10th	4.0
Present-Day 30th	10.1
Present-Day 50th	14.4
Present-Day 90th	33.7
Monsoon 10th	7.7
Monsoon 30th	15.9
Monsoon 50th	19.3
Monsoon 90th	91.4
Glacial-Transition 10th	11.8
Glacial-Transition 30th	25.8
Glacial-Transition 50th	35.3
Glacial-Transition 90th	68.6

Source: Extracted from unsaturated zone flow model results for the average upper boundary net infiltration over the repository footprint (SNL 2007a).

Table 3. Selected Net Infiltration Maps for the Post-10,000-Year Period

Post-10,000-Year Map (Percentile)	Target Average Net Infiltration Rate over Repository Footprint (mm/yr) <sup>a</sup>	Pre-10,000-Year Selected Match <sup>a</sup>	Average Net Infiltration rate over Repository Footprint (Table 1.2) (mm/yr)	Scaling Factor
10th	21.29	Present-Day 90th	33.7	0.63
30th	39.52	Glacial-Transition 50th	35.3	1.12
50th	51.05	Glacial-Transition 90th	68.6	0.74
90th	61.03	Monsoon 90th	91.4	0.67

Source: <sup>a</sup>SNL 2007a, Table 6.1-3.

## 2. COMMITMENTS TO NRC

None.

## 3. DESCRIPTION OF PROPOSED LA CHANGE

None.

## 4. REFERENCES

SNL (Sandia National Laboratories) 2007a. *UZ Flow Models and Submodels*. MDL-NBS-HS-000006 REV 03 AD 01. Las Vegas, Nevada: Sandia National Laboratories. ACC: DOC.20080108.0003.

SNL 2007b. *Calibrated Unsaturated Zone Properties*. ANL-NBS-HS-000058 REV 00. Las Vegas, Nevada: Sandia National Laboratories. ACC: DOC.20070530.0013.

SNL 2008. *Simulation of Net Infiltration for Present-Day and Potential Future Climates*. MDL-NBS-HS-000023 REV 01 AD 01. Las Vegas, Nevada: Sandia National Laboratories. ACC: DOC.20080201.0002.

## 5. LIST OF ATTACHMENTS

Electronic files containing net infiltration data along with spatial coordinates are provided as the following enclosures to the transmittal letter for this RAI response:

<b>Enclosure Number</b>	<b>File Name</b>
Enclosure 9	<i>PD_R2_V18_Infiltration.txt</i>
Enclosure 10	<i>PD_R1_V13_Infiltration.txt</i>
Enclosure 11	<i>PD_R1_V18_Infiltration.txt</i>
Enclosure 12	<i>PD_R2_V17_Infiltration.txt</i>
Enclosure 13	<i>MO_R1_V19_Infiltration.txt</i>
Enclosure 14	<i>MO_R1_V17_Infiltration.txt</i>
Enclosure 15	<i>MO_R1_V06_Infiltration.txt</i>
Enclosure 16	<i>MO_R2_V15_Infiltration.txt</i>
Enclosure 17	<i>GT_R1_V01_Infiltration.txt</i>
Enclosure 18	<i>GT_R1_V02_Infiltration.txt</i>
Enclosure 19	<i>GT_R2_V16_Infiltration.txt</i>
Enclosure 20	<i>GT_R1_V05_Infiltration.txt</i>

**RAI Volume 3, Chapter 2.2.1.3.5, First Set, Number 4:**

Justify the assumption(s) that soil and bedrock properties are invariant in the infiltration model over 10,000 years, given that this period includes three discrete climate states. This information is needed to evaluate compliance with 10 CFR 63.114(a)(1,2).

Basis: SAR Section 2.3.1.3.2.1.3 states that soil depth and properties are assumed to be constant for the next 10,000 years based on scientific judgment, but there does not appear to be any discussion of what the basis is for the scientific judgment in the SAR and supporting documents. In particular, it is not clear why soil properties (e.g., permeability, water holding capacity) would remain unaffected as climate changes over 10,000 years. Changed soil profiles may affect infiltration and overland flow patterns. There also does not appear to be any discussion in the SAR and supporting documents regarding how bedrock properties might change over the next 10,000 years, such as might occur because of fracture infill or dissolution of carbonates under wetter climatic conditions.

**1. RESPONSE**

Possible soil and bedrock property changes over the next 10,000 will not significantly increase predicted net infiltration. The surficial soils and underlying shallow bedrock above the Yucca Mountain repository have been exposed to repeated wet and dry climate cycles during the Pleistocene. These repeated cycles and combined effects of weathering, eolian deposition, and erosion have affected the soil and characteristics of rock currently at or near the surface. Potential changes in soil and rock characteristics and properties resulting from the projection of future climates over the next 10,000 years are not expected to significantly alter the properties of the surficial soils and underlying bedrock, and therefore are not expected to affect the predicted net infiltration rate. With the exception of the depth of soil depth class 4 and the water holding capacity of soil group 5/7/9 (SNL 2008a, Section 6.5.2.2[a]), uncertainty in hydrologic properties of surficial soil types and shallow bedrock has an insignificant effect on uncertainty in predicted net infiltration rate. Finally, uncertainty of the net infiltration maps used in the total system performance assessment (TSPA) is constrained by independent observations of temperature and chloride concentration using the unsaturated zone flow model (SNL 2007, Section 6.8.5). Because of this, it is reasonable to assume that uncertainty in soil and bedrock hydrologic properties considered in the net infiltration model includes any uncertainty associated with potential temporal variation in those properties over the next 10,000 years.

**1.1 POTENTIAL CHANGES IN SOIL PROPERTIES THAT COULD AFFECT NET INFILTRATION**

Of the nine different soil types mapped over the infiltration model domain, the majority of the infiltration model area and unsaturated zone model area is overlain by soil type 5, which covers 54% and 66% of the modeled areas, respectively (SNL 2008a, Table 6.5.2.2-2[a]). When similar soil types are grouped together, soil group 5/7/9 occurs over about 65% of the infiltration model domain and 81% of the unsaturated zone flow model domain. As illustrated in *Simulation of Net*

*Infiltration for Present-Day and Potential Future Climates* (SNL 2008a, Figure 6.5.2.2-2[a]), this soil group occurs over almost the entire footprint of the Yucca Mountain repository. In addition, this soil group corresponds to the shallow soil depth class 4, which dominates the predicted net infiltration (compare Figures 6.5.2.2-2[a], 6.5.2.4-1[a], and 6.5.7.3-2[a] through 6.5.7.3-5[a] of SNL 2008a). Therefore, soil type 5 is the most pervasive soil in the vicinity of Yucca Mountain and is the most significant soil type affecting infiltration over the repository block.

Soil type 5 is classified as colluvium consisting of rock fragments that have been separated from the parent rock by weathering processes, lacking fine-grained material at the surface and containing increasing silt and sand deposits of inferred eolian origin at depth. The age of this soil type is estimated as early to mid-Pleistocene, consistent with dating of the desert varnish on some rock fragments yielding ages of 800,000 years. Cycles of glacial and interglacial climates occur about every 100,000 years (BSC 2004, Section 7.1), which implies that the soils at Yucca Mountain have experienced about eight glacial and interglacial climate cycles in the last 800,000 years. The pedogenic processes that have occurred over the last several hundred thousand years have resulted in the observed soil characteristics, including soil hydraulic properties and soil texture. Although these processes are expected to continue for the next 10,000 years, the change in soil characteristics is expected to be minimal due to this small incremental increase in time compared to the total soil development time.

Pedogenic processes that are time dependent, such as the development of desert pavement, the accumulation of argillic materials, and the cementation of pedogenic carbonates, can potentially alter the hydraulic properties of soils at Yucca Mountain. However, the above time-dependent pedogenic processes would decrease the permeability and/or increase the water holding capacity of the soil horizon and would tend to slow the movement of infiltrating water through the soil. Slower water movement allows more time for evapotranspiration processes to remove water, thus decreasing the net infiltration rate. The development of soil hydraulic properties (based on the existing observed particle size distributions) overestimates the predicted net infiltration rate in those soil types where pedogenic processes may alter the hydraulic properties with time.

In addition to the soil hydraulic properties (notably the soil permeability and water holding capacity), the soil horizon depth may change over the next 10,000 years due to weathering and erosion processes associated with future climate changes. The potential effects of these processes were evaluated in the exclusion basis for the features, events, and processes (FEPs) 1.2.07.01.0A (Erosion/Denudation) and 1.2.07.02.0A (Deposition). These effects did not significantly affect the predicted net infiltration rate, or performance assessments conducted to demonstrate compliance with 10 CFR 63.311, 63.321, or 63.331, on the basis of low consequence (SNL 2008b, FEPs 1.2.07.01.0A and 1.2.07.02.0A). Although long-term erosion rates (ranging from 0.2 to 6 cm/10,000 years) (Stuckless and Levich 2007, p. 84) may remove unconsolidated materials and decrease soil depth, the climate in the next 10,000 years is expected to be generally wetter than present-day, favoring the production of colluvial deposits rather than the erosion and redistribution of these deposits, which takes place during drier climates when hillslopes are not as stabilized by vegetation (SNL 2008b, FEP 1.2.07.02.0A). Because the production of colluvial materials is favored over the next 10,000 years (because 9,400 of the next 10,000 years are projected to be wetter than present-day conditions (BSC 2004, Section 7.1)),

there will likely be a net increase in colluvial materials over the repository horizon over that time, increasing the soil depth and decreasing predicted net infiltration. Therefore, assuming soil properties remain constant provides an approach that estimates infiltration that is expected to be bounding for assessments of performance.

## **1.2 POTENTIAL CHANGES IN BEDROCK PROPERTIES THAT COULD AFFECT NET INFILTRATION**

The uncertainty in bedrock saturated hydraulic conductivity used in the prediction of net infiltration at Yucca Mountain has been addressed by considering a range of values between a lower bound represented by assuming all the fractures are 100% filled by caliche, and an upper bound represented by assuming all the fractures are partially filled and have an additional aperture of 200 microns. This range was developed to address the uncertainty in the proportion of fractures that are unfilled and the hydraulic aperture of the unfilled fractures in the bedrock immediately below the surficial soils. The available data from the Alcove 1 infiltration test, another infiltration test at Fran Ridge, and an analysis of fracture air-permeability data and fracture frequency data indicate that this range is reasonable.

The predicted net infiltration considered that all bedrock infiltration hydrogeologic units (except units 405 and 406) used the mean of the hydraulic conductivity distribution, which is substantially controlled by the assigned upper bound of the log-uniform distribution. The uncertainty in the saturated hydraulic conductivity of bedrock infiltration hydrogeologic units 405 and 406 was treated explicitly in the model because these units comprise more than 15% of the unsaturated zone model area or repository footprint (SNL 2008a, Tables 6.5.2.5-1[a] and I-1). The use of fixed values of saturated hydraulic conductivity for all other infiltration hydrogeologic units did not under-represent the mean or uncertainty in the predicted net infiltration over the unsaturated zone model area. This is based on the fact that the other bedrock infiltration hydrogeologic units have low influence on net infiltration because they constitute less than 15% of the unsaturated zone model area. In addition, the lowest mean hydraulic conductivity for these bedrock units ( $7.7 \times 10^{-7}$  m/s or 67 mm/day) is greater than the nominal saturated hydraulic conductivity of the overlying soil group 5/7/9 ( $6.8 \times 10^{-7}$  m/s or 59 mm/day) covering most of the unsaturated zone model domain, and will not impede net infiltration (SNL 2008a, Tables 6.5.2.2-2, 6.5.2.3-1, and 6.5.2.6-1). Any potential increase in the mean hydraulic conductivity due to climate change and corresponding dissolution of carbonates in the caliche fracture infilling would not affect the predicted net infiltration because the overlying soil units control the water movement rate. Similarly, any potential decrease in the mean hydraulic conductivity due to climate change and corresponding precipitation of caliche in partially filled fractures would tend to decrease the predicted net infiltration.

The uncertainty in the hydraulic conductivity of bedrock units 405 and 406 encompasses a broad range of values (for example, a minimum of  $2.1 \times 10^{-8}$  m/s or 1.8 mm/day and a maximum of  $7.7 \times 10^{-6}$  m/s or 670 mm/day for unit 406), from less than to greater than the saturated hydraulic conductivity of soil group 5/7/9 (59 mm/day) (SNL 2008a, Tables 6.5.2.3-1 and 6.5.2.6-1). Note that these lower and upper hydraulic conductivity values (e.g., for unit 406) are also higher than the lower and upper values, respectively, of daily precipitation events, which are about 0 to about 75 mm/day (SNL 2008a, Figures 6.5.1.7-1[a] to 6.5.1.7-4[a]). When sampled bedrock hydraulic

conductivity is greater than the soil saturated hydraulic conductivity or the rate of infiltration through the soil, the bedrock does not impede net infiltration through the bedrock. When the sampled bedrock hydraulic conductivity is less than the soil saturated hydraulic conductivity and less than the rate of infiltration through the soil (which is limited by the soil saturated hydraulic conductivity), then the bedrock may impede net infiltration because the soil would saturate and potentially pond, allowing the water to run off to other grid cells and potentially not infiltrate.

Any potential increase in the bedrock hydraulic conductivity of units 405 and 406 due to climate change and corresponding dissolution of carbonates in the caliche fracture infilling would only potentially affect the predicted net infiltration for the lower end of the sampled hydraulic conductivity distribution. However, this effect is expected to be small as shown in the extended sensitivity analysis (SNL 2008a, Section 7.1.4) because: (1) these units comprise less than half of the unsaturated zone model area (SNL 2008a, Table 6.5.2.5-1) and (2) about half of the sampled hydraulic conductivity distribution would be sufficiently high that either the saturated hydraulic conductivity of the overlying soil or the infiltration flow rate through the soil would control the net infiltration. Similarly, any potential decrease in the bedrock hydraulic conductivity due to climate change and a corresponding precipitation of caliche in partially filled fractures would tend to decrease the predicted net infiltration.

### **1.3 SIGNIFICANCE OF SOIL AND BEDROCK PROPERTIES ON INFILTRATION UNCERTAINTY**

The soil properties that could potentially affect the prediction of net infiltration in the infiltration model include soil depth, soil hydraulic conductivity, soil saturated water content, and soil water holding capacity. Of these properties, the predicted uncertainty in net infiltration has been determined to be significantly affected by the uncertainty in the soil depth of soil depth class 4 and to a lesser extent the uncertainty in the water holding capacity of soil group 5/7/9 (SNL 2008a, Section 6.7.2 and Appendix H). The importance of soil thickness is also illustrated by noting that the spatial distribution of soil depth class 4 correlates with the spatial distribution of areas with significant predicted net infiltration, while soil depth classes 1 (very deep soils), 2 (moderately deep soils), and 3 (intermediate depth soils) have very little predicted net infiltration (SNL 2008a, Figures 6.5.2.4-1[a] and 6.5.7.3-2[a] to 6.5.7.3-5[a], respectively, as well as Tables 6.5.7.6-1[a] and 6.5.7.6-2[a]). The uncertainty analyses indicate that increasing the soil depth or the water holding capacity tends to decrease the predicted net infiltration. Because temporal changes in soil properties with future, wetter climate changes are likely to increase the soil depth and water holding capacity because of soil stabilization by vegetation, these changes will decrease the predicted net infiltration.

The only bedrock property that potentially affects the prediction of net infiltration in the infiltration model is the bedrock permeability or hydraulic conductivity. Uncertainty in the hydraulic conductivity of bedrock infiltration hydrogeologic units 405 and 406 was not a significant factor in the uncertainty in the predicted net infiltration (SNL 2008a, Appendix H) over either the entire infiltration model domain or the unsaturated zone model area. This result can be explained by both the small fraction of total infiltration area overlain by these two units, 23% and 19%, respectively (SNL 2008a, Table 6.5.2.5-1), and/or the observation that most of the

uncertainty distribution of saturated hydraulic conductivity is sufficiently high to not impede net infiltration.

The potential effect of bedrock properties on net infiltration would be significant if the bedrock hydraulic conductivity is sufficiently smaller than the overlying soil saturated hydraulic conductivity or if there is a significant area with no soil cover. In these situations, the infiltration event could either run off as overland flow or interflow along the soil bedrock interface or increase the water saturation in the soil column. The possibility of overland flow is considered in the Mass Accounting System for Soil Infiltration and Flow (MASSIF) model and generally leads to a reduction in predicted net infiltration as water migrates from side slopes to washes with greater soil depth leading to increased vegetative cover and thus an increase in evapotranspiration. The possibility of interflow has been assumed to be insignificant in the MASSIF model, in part because the bedrock hydraulic conductivities, which include the assumed effects of partially filled fractures, tend to be significantly higher than the hydraulic conductivities of the overlying soils (SNL 2008a, Section 5.1). In addition, the means of the distribution of bulk bedrock hydraulic conductivities (assumed to be log-uniform from the lower bound, which treats all fractures as completely filled, to the upper bound, which adds an additional 200-micron unfilled aperture to each fracture) are all greater than  $7.7 \times 10^{-7}$  m/s (or 67 mm/day), which is considerably greater than most precipitation events expected at Yucca Mountain (SNL 2008a, Table 6.5.2.6-1 and Figures 6.5.1.7-1[a] to 6.5.1.7-4[a]). Therefore, using the mean hydraulic conductivity of the bedrock, the upper bound of which includes the effect of each fracture having an additional 200-micron unfilled aperture, maximizes the amount of net infiltration predicted in the MASSIF model. Any potential future changes in degree of caliche plugging in the bedrock would only tend to decrease the predicted net infiltration.

#### **1.4 SIGNIFICANCE OF INFILTRATION UNCERTAINTY ON TSPA UNCERTAINTY**

The uncertainty in the predicted net infiltration rate, as represented by net infiltration maps corresponding to the 10th, 30th, 50th, and 90th percentiles of the cumulative distribution, is one input to the unsaturated zone flow model. The unsaturated zone flow model is used to produce estimates of the spatial distribution of percolation flux: (1) at the base of the PTn hydrostratigraphic unit; (2) at the repository horizon; and (3) below the repository horizon. These estimates provide the expected flow fields and flow paths from the repository to the water table, as well as the uncertainty in the unsaturated zone flow conditions, for use as input to the TSPA. The predicted unsaturated zone flow fields include additional modifications to the probabilities of individual infiltration maps by constraining predicted flow fields with independent observations of temperature and chloride concentrations in the unsaturated zone. These modifications are implemented using the Generalized Likelihood Uncertainty Estimation (GLUE) methodology (SNL 2007, Section 6.8.5). The revised (i.e., posterior) weights based on applying this methodology are 61.91%, 15.68%, 16.45%, and 5.96%, respectively, for the 10th, 30th, 50th, and 90th percentile infiltration maps (SNL 2007, Table 6.8-1).

Changes in predicted net infiltration related to soil or bedrock properties, if they were to occur and be propagated to the prediction of unsaturated zone flow, may be conceptualized as modifying the prior weights for the individual net infiltration maps. Even if the prior weights change, the GLUE-derived posterior weight is not expected to be significantly modified because

the likelihood values are expected to change and compensate for the prior weight change. That is, the posterior weight is not significantly sensitive to the uncertainty in the prior weight. Therefore, small changes in prior weights, which may be the result of including the effects of temporal changes in soil or bedrock properties, are not expected to change the unsaturated zone flow model results used in the TSPA. Based on the analyses presented in the response to RAI 3.2.2.1.3.6-007, large changes in weights used in the TSPA model are not expected to significantly affect repository performance.

## 1.5 SUMMARY AND CONCLUSIONS

Insignificant changes in soil and bedrock properties are expected over the next 10,000 years due to climate. If they occur, changes in soil properties, notably the soil depth and water holding capacity, are expected to lead to a slight decrease in predicted net infiltration. Changes in bedrock properties, notably the bedrock hydraulic conductivity, would not change the predicted net infiltration because the mean hydraulic conductivity is dominated by the assumption that, at the upper bound, all fractures are partially filled with caliche and have an additional 200-micron unfilled aperture, thus not impeding net infiltration. Even if net infiltration rates did change due to changes in soil or bedrock properties, the use of the GLUE methodology to develop posterior weights would minimize the significance of these changes on the TSPA results.

In summary, the effects of temporal changes in soil and bedrock properties would not significantly change the inputs to the TSPA model or the TSPA results.

## 2. COMMITMENTS TO NRC

None.

## 3. DESCRIPTION OF PROPOSED LA CHANGE

None.

## 4. REFERENCES

BSC (Bechtel SAIC Company) 2004. *Future Climate Analysis*. ANL-NBS-GS-000008 REV 01 Las Vegas, Nevada: Bechtel SAIC Company. ACC: DOC.20040908.0005; DOC.20080813.0003.

SNL (Sandia National Laboratories) 2007. *UZ Flow Models and Submodels*. MDL-NBS-HS-000006 REV 03 AD 01. Las Vegas, Nevada: Sandia National Laboratories. ACC: DOC.20080108.0003; DOC.20080114.0001; LLR.20080414.0007; LLR.20080414.0033; LLR.20080522.0086; DOC.20090330.0026<sup>a</sup>.

SNL 2008a. *Simulation of Net Infiltration for Present-Day and Potential Future Climates*. MDL-NBS-HS-000023 REV 01 ADD 01. Las Vegas, Nevada: Sandia National Laboratories. ACC: DOC.20080201.0002; LLR.20080507.0008; LLR.20080522.0101.

ENCLOSURE 2

Response Tracking Number: 00391-00-00

RAI: 3.2.2.1.3.5-004

SNL 2008b. *Features, Events, and Processes for the Total System Performance Assessment: Analyses*. ANL-WIS-MD-000027 REV 00. Las Vegas, Nevada: Sandia National Laboratories. ACC: DOC.20080307.0003; DOC.20080407.0009; LLR.20080522.0166; DOC.20080722.0002.

Stuckless, J. and Levich, R. 2007. *The Geology and Climatology of Yucca Mountain and Vicinity, Southern Nevada and California*. Memoir 199. Boulder, Colorado: Geological Society of America.

NOTE: <sup>a</sup>Provided as an enclosure to letter from Williams to Sulima dtd 6/01/09, “Yucca Mountain – Request for Additional Information – Safety Evaluation Report, Volume 3 – Postclosure Chapter 2.2.1.3.6 – Flow Paths in the Unsaturated Zone, Set 1 – (Department of Energy’s Safety Analysis Report Sections 2.3.2 and 2.3.3).”

**RAI Volume 3, Chapter 2.2.1.3.5, First Set, Number 5:**

Explain why the infiltration model results appear to be less sensitive to mean annual precipitation than indicated in the supporting information used for post-model-development validation (e.g., SAR Figure 2.3.1-48). This information is needed to evaluate compliance with 10 CFR 63.114(a)(7).

Basis: Power law relationships between mean annual precipitation (MAP) and mean annual infiltration (MAI) from various researchers are reported in SAR Figure 2.3.1-48. The Wilson and Guan (2004) linearization of the Maxey Eakin relationship and the Faybishenko (2007) relationship between climate and infiltration (based on the meteorological stations used in the SAR to represent climate states) imply a rate of increase in MAI with respect to MAP. Using these relationships to scale the present day MAI values from SAR Table 2.3.1-2 implies that the monsoon and glacial transition values of MAI would be approximately 3 times larger than the values in SAR Tables 2.3.1-3 and 2.3.1-4. It is not clear why the MASSIF infiltration model does not exhibit a similar sensitivity to climate as these relationships.

**1. RESPONSE**

While the Mass Accounting System for Soil Infiltration and Flow (MASSIF) infiltration model results appear to be less sensitive to mean annual precipitation (MAP) than six of the seven comparison models used for model validation as presented in SAR Figure 2.3.1-48 alone, comparison of MASSIF results to a significant set of analogue data indicates reasonable agreement of MAP and mean annual infiltration (MAI) relationships. These seven comparison models are: the original Maxey-Eakin model (1950), two modified Maxey-Eakin (MME) models (DOE 1997; Nichols 2000), the Maxey-Eakin fit of Wilson and Guan (2004), two empirical models of Maurer and Berger (1997) and Faybishenko (2007), and the MAP/MAI equation attributed to Davisson and Rose in Faybishenko (2007). As discussed in SAR Section 2.3.1.3.4.2.2, the empirical model of Maurer and Berger (1997) represents MAP versus water yield, where water yield equals subsurface flow plus surface runoff, so it is not directly comparable to the MASSIF model results.

The model validation discussed in the infiltration model report (SNL 2008) provides a thorough set of comparisons, using a variety of methods, between the MASSIF model results and other researchers' models and data for sites in Nevada, the southwestern United States (New Mexico, west Texas, and southeast Arizona), and on the Columbia Plateau (centered in southeast Washington state). These comparisons are presented in Figures 7.2.1.2-1[a], 7.2.1.2-2[a], 7.2.1.2-3, and 7.2.1.2-4[a] of the infiltration model report (SNL 2008). All data from these four figures have been compiled into Figure 1 for this RAI response.

Figure 2 is similar to Figure 1, except that the Maurer and Berger (1997) model and all but one of the other six empirical models have been deleted, leaving only the Wilson and Guan (2004) fit of the Maxey-Eakin model for reference. All published data points using the Maxey-Eakin and MME methods have also been removed in Figure 2. Figure 2 reveals that the MASSIF model

results are fairly consistent with the range and trend of scatter of MAI/MAP data points. Figure 2 suggests that the MASSIF model results are corroborated by a variety of infiltration estimates including chloride mass balance estimates, water balance estimates, and calibrated model estimates. While the Maxey-Eakin and MME models are useful for comparison due to the historical significance of the well-recognized and nearly 60-year-old Maxey-Eakin model, comparison of Figures 1 and 2 suggests that the Maxey-Eakin and MME models appear to generally underestimate MAI at MAP values less than 300 mm/yr when compared to other published infiltration and recharge estimates for the western U.S. In addition, Figure 1 suggests that the two Faybishenko (2007) empirical models also generally underestimate MAI at MAP values less than 300 mm/yr.

The MASSIF infiltration model results are less sensitive to MAP than the comparison models used for model validation, as presented in SAR Figure 2.3.1-48 alone (excluding Maurer and Berger (1997)), and the monsoon and glacial transition values of MAI should be approximately three times larger if the MASSIF present-day climate results are expected to parallel the trend of six of the seven comparison models (as noted above, the Maurer and Berger model (1997) is not directly comparable). However, this is not the case. The general trend of the MASSIF model results does not precisely follow the trend of the six comparison models from SAR Figure 2.3.1-48 for several reasons. The Maxey-Eakin and MME models are based on large-scale relationships between MAP and recharge for basins in Nevada that are dominated by thick soils (where increased evapotranspiration decreases infiltration), whereas the MASSIF model domain is dominated by highlands with thin soils. This difference between basin-scale versus single-mountain-scale has also been identified by the Center for Nuclear Waste Regulatory Analysis (Stofhoff and Musgrove 2006, p. 14):

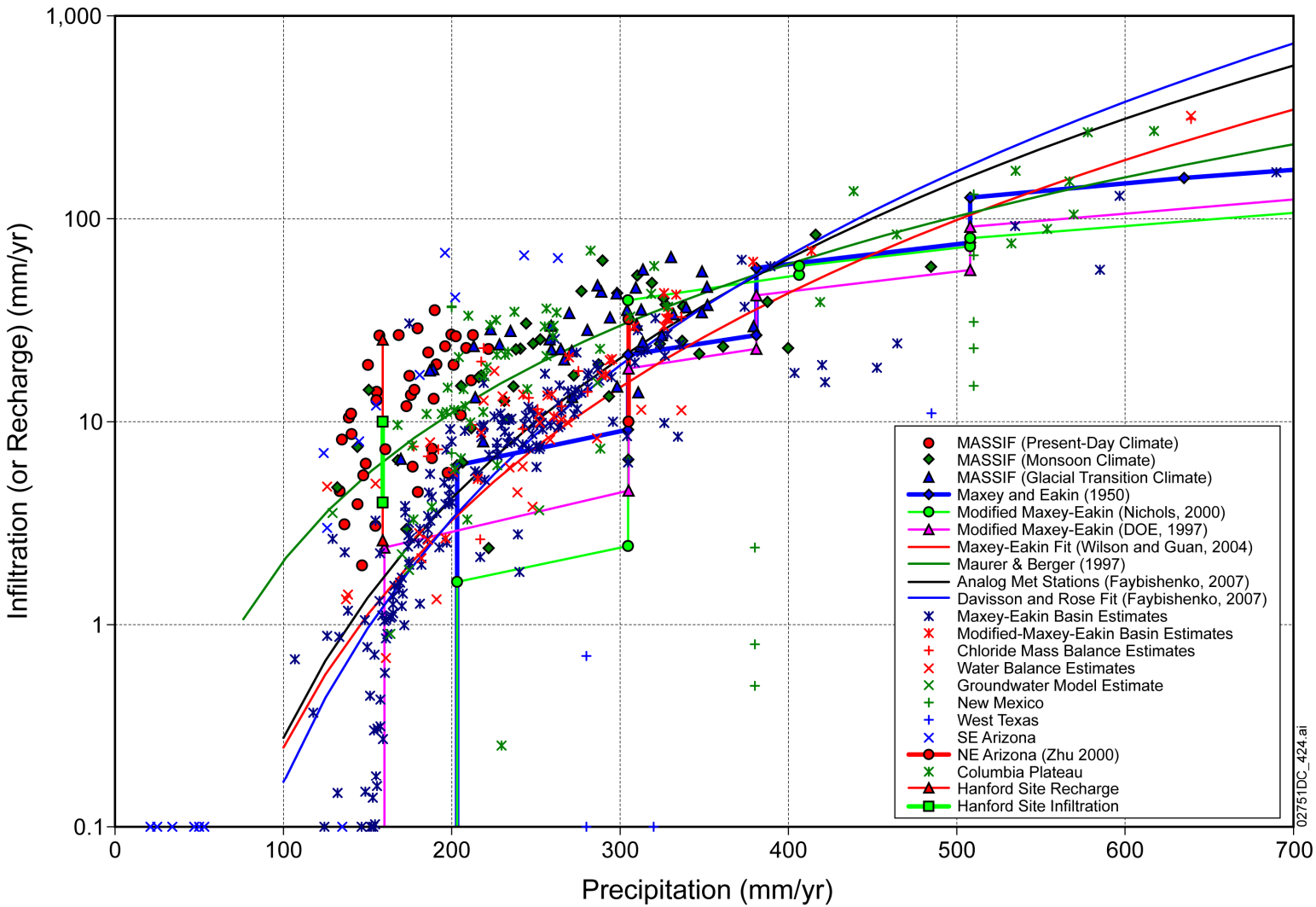
The relationship between basin-average precipitation and basin-average recharge appears to differ from the relationship between precipitation and recharge at a smaller scale, particularly in mountainous regions. Since Yucca Mountain covers only a small fraction of the area of a typical Great Basin hydrologic basin, estimates of recharge as a fraction of precipitation at the scale of an entire hydrologic basin may be a misleading basis for estimating recharge at Yucca Mountain.

The Maxey-Eakin and MME models do not include any model or parameter uncertainty, while the MASSIF model results incorporate considerable parameter and climate uncertainties that result in the scatter of the MASSIF data points. The MASSIF model results also include three distinct climate states that are not incorporated into the Maxey-Eakin and MME models. It is the combination of these factors that result in the MASSIF model results deviating from the trend of the six models shown in SAR Figure 2.3.1-48.

In addition, although the MASSIF model results are corroborated by the many data points in Figure 2, the MASSIF model results are conservative in that the mean of the 40 realizations of MAI for a given climate overestimate net infiltration. Key conservatisms are discussed in SAR Section 2.3.1.4 and include: (1) soil depth of the shallow soil depth class; (2) soil water holding capacity (also see the response to RAI 3.2.2.1.3.5-008); (3) bedrock  $K_{sat}$  (also see the response to RAI 3.2.2.1.3.5-008); and (4) the lack of a mechanism to remove water from bedrock (i.e., via

plant roots). Weighting factors are calculated using the generalized likelihood uncertainty evaluation (GLUE) methodology as discussed in SAR Section 2.3.2.4.1.2.4.5. These weighting factors effectively act to calibrate net infiltration to temperature and chloride data in the unsaturated zone.

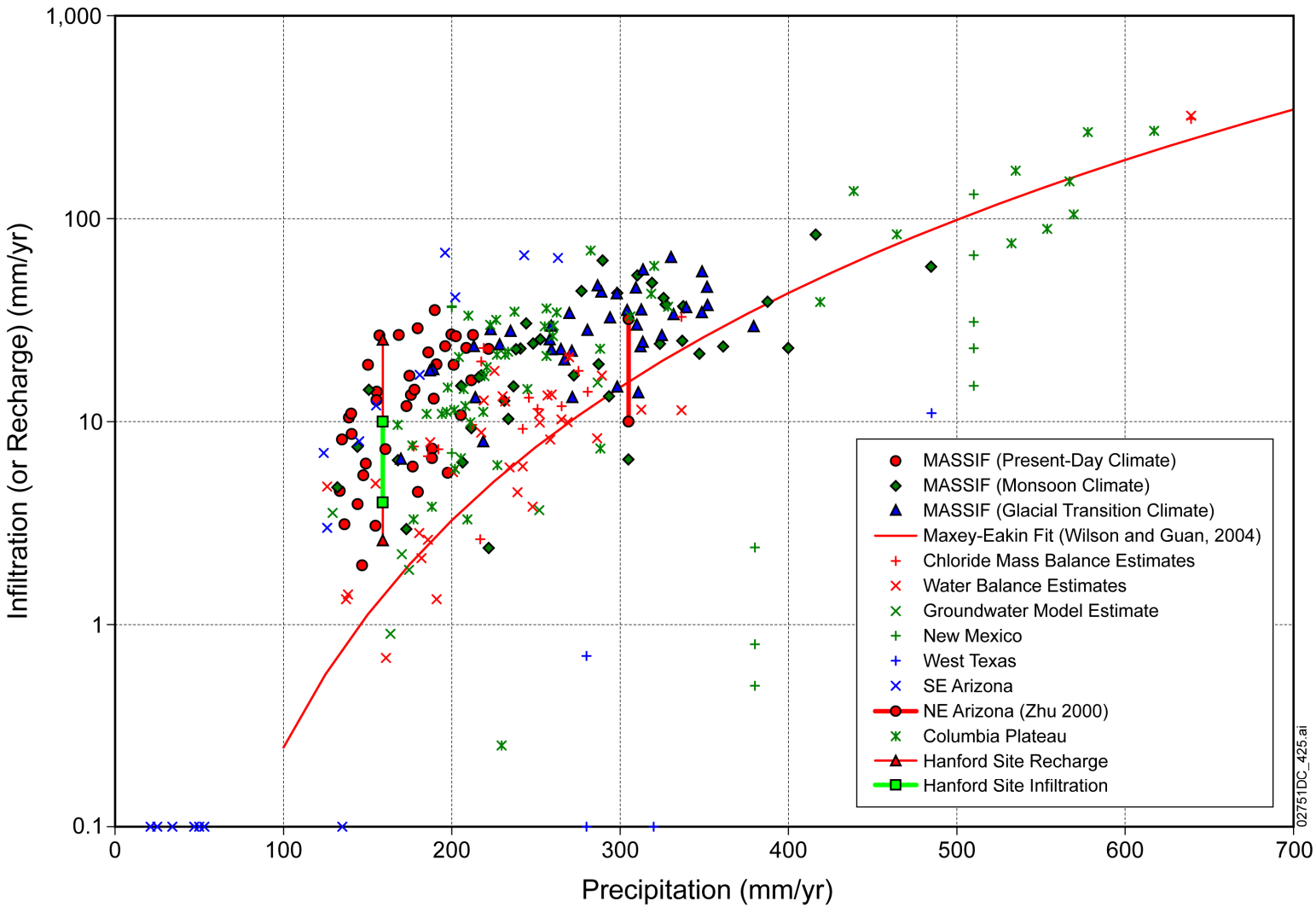
The MASSIF model results are less sensitive to MAP than six of the seven models presented in SAR Figure 2.3.1-48. However, comparison of the MASSIF model results to all corroboration data points from the infiltration model report (SNL 2008), and removal of the Maxey-Eakin and MME models and data points and empirical models, reveals that the MASSIF model results compare well to several different data sets which supports model validation (SNL 2008, Section 7.2). In addition to the comparison of MASSIF results to data discussed above, the MASSIF model and its results have been validated by several other methods (SAR Section 2.3.1.3.4).



02751DC\_424.ai

NOTE: No data points are hidden by the legend box, but one data point for the Columbia Plateau is not shown (MAP = 956, MAI = 383 mm/yr).

Figure 1. Comparison of Recharge Estimates for All Models and Data from Infiltration Report (SNL 2008) with MASSIF Model Results



NOTE: No data points are hidden by the legend box, but one data point for the Columbia Plateau is not shown (MAP = 956, MAI = 383 mm/yr).

Figure 2. Comparison of Recharge Estimates for Selected Models and Data from Infiltration Report (SNL 2008) with MASSIF Model Results

## 2. COMMITMENTS TO NRC

None.

## 3. DESCRIPTION OF PROPOSED LA CHANGE

None.

## 4. REFERENCES

DOE (U.S. Department of Energy) 1997. *Regional Groundwater Flow and Tritium Transport Modeling and Risk Assessment of the Underground Test Area, Nevada Test Site, Nevada*.

DOE/NV-477. Las Vegas, Nevada: U.S. Department of Energy. ACC: MOL.20010731.0303.

Faybishenko, B. 2007. "Climatic Forecasting of Net Infiltration at Yucca Mountain Using Analogue Meteorological Data." *Vadose Zone Journal*, 6, 77-92. Madison, Wisconsin: Soil Science Society of America.

Maurer, D.K. and Berger, D.L. 1997. *Subsurface Flow and Water Yield from Watersheds Tributary to Eagle Valley Hydrographic Area, West-Central Nevada*. Water-Resources Investigations Report 97-4191. Carson City, Nevada: U.S. Geological Survey. ACC: MOL.20060808.0017.

Maxey, G.B. and Eakin, T.E. 1950. *Ground Water in White River Valley, White Pine, Nye, and Lincoln Counties, Nevada*. Water Resources Bulletin No. 8. Carson City, Nevada: State of Nevada, Office of the State Engineer.

Nichols, W.D. 2000. *Regional Ground-Water Evapotranspiration and Ground-Water Budgets, Great Basin, Nevada*. U.S. Geological Survey Professional Paper 1628. Reston, Virginia: U.S. Geological Survey. ACC: LLR.20070213.0076.

SNL (Sandia National Laboratories) 2008. *Simulation of Net Infiltration for Present-Day and Potential Future Climates*. MDL-NBS-HS-000023 REV 01 AD 01. Las Vegas, Nevada: Sandia National Laboratories. ACC: DOC.20080201.0002; LLR.20080507.0008; LLR.20080522.0101.

Stothoff, S. and Musgrove, M. 2006. Literature Review and Analysis: Climate and Infiltration. CNWRA 2007-002. San Antonio, Texas: Center for Nuclear Waste Regulatory Analyses. ACC: LLR.20070725.0015.

Wilson, J.L. and Guan, H. 2004. "Mountain-Block Hydrology and Mountain-Front Recharge." In *Groundwater Recharge in a Desert Environment: The Southwestern United States*. Hogan, J.F.; Phillips, F.M.; and Scanlon, B.R., eds. Water Science and Application 9. Pages 113-137. Washington, D.C.: American Geophysical Union.

**RAI Volume 3, Chapter 2.2.1.3.5, First Set, Number 6:**

Describe the consequences to repository performance if the net infiltration patterns were consistent with the variant property set estimated for Pagany Wash. This information is needed to evaluate compliance with 10 CFR 63.114(a)(2).

Basis: The infiltration model appears to emphasize distributed net infiltration (only the present day 50th percentile map out of the 12 realizations in SAR Figures 2.3.1-26 through 2.3.1-29 and 2.3.1-31 through 2.3.1-38 has channel infiltration at least comparable to distributed infiltration). However, SAR Section 2.3.1.3.4.1 describes a confidence building exercise using observations from Pagany Wash in which a simulation with alternative properties derived from field observations yielded more channel infiltration and less distributed infiltration than a simulation with nominal properties, with an almost identical areal average infiltration and a closer match to field observations. SAR Section 2.3.1.3.3.1.2 and SNL (2007, Section 7.1.3.2) describe simulations of the entire model domain using the variant property set. Simulations with the variant property set tend to indicate similar total infiltration but with distinctly increased channel infiltration compared to the corresponding simulations with the base case properties.

It is not clear from SAR Section 2.3.1.3.4.1 why the areal average infiltration is the same with both property sets. For example, the result could be a consequence of a fortuitous selection of changed properties, or it could be a more general result that increased hillslope runoff (regardless of generating mechanism) is simply recaptured as channel infiltration. SAR Section 2.3.1.4 explains that, to a certain extent, input properties were chosen to conservatively not restrict infiltration, which may tend to result in systematically reduced runoff estimates. For example, bedrock permeability in most units does not limit simulated infiltration because of assumed fracture properties, but bedrock fracture properties are highly uncertain and reduced fracture permeability may act like the reduced soil conductivity in the variant property set by promoting runoff.

It is not clear that repository performance is not overestimated using a set of input properties that emphasizes distributed infiltration over channel (localized) infiltration even if the areal average infiltration is similar. Infiltration patterns dominated by localized infiltration may result in an overall greater percentage of percolation flux at the repository horizon becoming seepage. Relatively large and frequent wetting pulses from channels may be more likely to locally penetrate the PTn in transient pulses by maintaining locally damp conditions in the PTn, increasing seepage relative to steady percolation. Further, because the washes are much larger in the north, the two geomorphic regions (north and south of Drill Hole Wash) described in SAR Section 2.3.1.3.1.3 may have different consequences for repository performance. For example, total net infiltration over the repository footprint may increase if upstream runoff in large washes, such as Drill Hole Wash, moves into the footprint and induces substantial channel infiltration.

## 1. RESPONSE

### 1.1 BACKGROUND

Maps showing mean annual net infiltration (MAI) are presented in: SAR Figures 2.3.1-26 to 2.3.1-29 for present-day climate, SAR Figures 2.3.1-31 to 2.3.1-34 for monsoon climate, and SAR Figures 2.3.1-35 to 2.3.1-38 for glacial-transition climate. There are four figures for each climate, corresponding to the 10th, 30th, 50th, and 90th percentile infiltration maps from the total of 40 realizations per climate. These are the base-case infiltration maps and are the result of sampling important uncertain parameters using a Latin Hypercube Sampling methodology (SNL 2008, Section 6.5.6.1).

SAR Section 2.3.1.3.4.1 and *Simulation of Net Infiltration for Present-Day and Potential Future Climates* (SNL 2008, Sections 7.1.3, 7.1.3.1, and 7.1.3.2[a]) describe the Mass Accounting System for Soil Infiltration and Flow (MASSIF) model validation activities related to matching model results to streamflow and infiltration data. In the first activity (SNL 2008, Section 7.1.3), soil  $K_{sat}$  for all types was decreased uniformly until MASSIF model streamflow output reasonably matched the streamflow data (see, for example, SAR Figure 2.3.1-46). In the second activity (SNL 2008, Section 7.1.3.1), soil  $K_{sat}$  was decreased for most soil types, soil  $K_{sat}$  was increased for soil type 3 (which is the dominant soil type found in most channels; see Figure 6.5.2.2.1[a] in SNL 2008), and rock  $K_{sat}$  was increased so as not to be limiting, to be consistent with a second case (SNL 2008, Section 7.2.1.1.2[a]) in which MASSIF  $K_{sat}$  values were adjusted to match reported infiltration at borehole UZ #4 (LeCain et al. 2002). These adjustments to soil and rock  $K_{sat}$  values comprise the variant case property set. In the third activity (SNL 2008, Section 7.1.3.2[a]), the adjustments described for the second activity (using the Pagany Wash variant case property set), were applied to the entire MASSIF model domain.

The results of the first activity showed that soil  $K_{sat}$  had to be decreased by factors ranging from 0.3 to 0.7 to match streamflow data (SNL 2008, Section 7.1.3). The results of the second and third activities indicated that while the application of the Pagany Wash variant parameter set changed the spatial distribution of runoff versus infiltration, it had very little effect on the spatial averages of net infiltration, or the fraction of runoff. SAR Figure 2.3.1-27 and Figure 7.1.3.2-2[a] of *Simulation of Net Infiltration for Present-Day and Potential Future Climates* (SNL 2008) show the present-day 30th percentile net infiltration maps for the base case and the variant soil  $K_{sat}$  case, respectively. In the base-case figure (SAR Figure 2.3.1-27), infiltration is relatively higher in the highlands (areas dominated by thin soils and no channels) and relatively lower in the stream channels compared to the variant case figure (SNL 2008, Figure 7.1.3.2-2[a]). Despite these differences in the spatial distribution of net infiltration, the average net infiltration and runoff results for the entire model domain, the unsaturated zone model domain, and the repository footprint, are similar between the cases (see SNL 2008, Table 7.1.3.2-1[a]).

## 1.2 BASE CASE VERSUS VARIANT CASE INFILTRATION AND RUNOFF

Drill Hole Wash is the second largest watershed in the MASSIF model domain, with an area of 40.6 km<sup>2</sup>, covering much of the repository footprint (see dark green portion of SAR Figure 2.3.1-45). Using Site 3 precipitation data for water years 1994 through 1998 (SNL 2006), the 5-year total runoff that leaves the Drill Hole Wash domain for the base case and variant case is  $8.17 \times 10^5$  and  $4.24 \times 10^5$  m<sup>3</sup> (663 and 344 acre-feet), respectively. The total runoff is 1.9 times higher for the base case than the variant case. Despite increased runoff into stream channels for the variant case, the increased soil  $K_{sat}$  in channels results in increased infiltration into the channels, with a net decrease in runoff out of the model domain. MAI for this comparison was 5.52 and 5.89 mm/yr for the base case and variant case, respectively. Therefore, the base case and variant case represent two extremes of spatial distribution of net infiltration: the base case having distributed net infiltration, and the variant case having localized net infiltration. Areal averages of infiltration for the base case and variant case are similar because increased hillslope runoff is recaptured as channel infiltration.

## 1.3 EFFECT OF BASE CASE VERSUS VARIANT CASE PROPERTIES ON REPOSITORY PERFORMANCE

The RAI mentions two situations that could increase channel infiltration in the model results: (1) bedrock fracture properties are uncertain, and reduced bedrock permeability may have an effect similar to reduced soil conductivity, promoting runoff into channels; and (2) channel flow from upstream may flow into channels within the repository footprint. Both of these mechanisms are included in the variant case. The variant property set applies a relatively large value for the uniform bedrock  $K_{sat}$  of 0.001 m/s (86 m/day) to every grid cell, which ensures that there is no slowing of infiltration at the soil–bedrock interface. At the same time, the reduction of soil  $K_{sat}$  values for all but soil type 3 increases runoff, ensuring that streamflow data are matched, and promoting infiltration in channels. The simulation includes the watersheds upstream from the repository footprint. Accordingly, the variant case is a good choice for evaluating the effect of focused infiltration in channels on repository performance.

Two approaches are used to evaluate the effect of focused infiltration on repository performance: (1) comparison of channel infiltration in the variant case with earlier analysis of the damping of infiltration transients by the Paintbrush nonwelded hydrogeologic (PTn) unit (see the response to RAI 3.2.2.1.2.1-5-005) to evaluate the effects of temporal variability in infiltration; and (2) comparison to a previous evaluation of flow focusing in the unsaturated zone, which demonstrated that repository performance is not sensitive to spatial variability in seepage (see the response to RAI 3.2.2.1.3.6-006).

### 1.3.1 Temporal Damping of Channel Infiltration

Net infiltration in channels (soil type 3) simulated for the variant case is generally less than the infiltration boundary condition used to demonstrate temporal damping in the PTn unit. To show this relationship, the analysis that follows is based on the variant case corresponding to the present-day 90th percentile base-case infiltration map summarized in SAR Table 2.3.1-20. The MASSIF model domain contains 16,514 grid cells with soil type 3 (approximately 12% of the

model domain), which is the type that generally corresponds to channels (SNL 2008, Table 6.5.2.2-2[a]). Using the present-day 90th percentile results, MAI for the channel grid cells is 0.5 and 51.0 mm/yr for the base case and variant case, respectively. MAI for the entire model domain for this realization is 26.7 and 27.2 mm/yr for the base case and variant case, respectively (SAR Table 2.3.1-20). The MASSIF model calculates MAI by summing the product of MAI for a representative year times its weight (see SAR Tables 2.3.1-10, 2.3.1-11, and 2.3.1-12). In this manner, MASSIF can simulate low and high frequency precipitation years using only ten representative years. Table 1 (columns 3 and 4) shows the base-case and variant-case channel infiltration calculated for the 10 representative years calculated using the MASSIF model (SNL 2008). Columns 5 and 6 show the weighted channel infiltration values that account for the frequency of each of the ten representative years. Summing these values in columns 5 and 6 yields MAI.

The weighted values of channel infiltration in Table 1 were used to generate cumulative distribution functions (CDFs) for channel infiltration. Then, stochastic 1,000-year records of channel infiltration for the base case and variant case were generated by randomly sampling the CDFs. Figure 1 shows the CDFs of spatially averaged net infiltration generated for base-case and variant-case channel infiltration (soil type 3 only) using the data from columns 5 and 6 of Table 1. Also shown are CDFs for the overall model domain (all locations and soil types), which show that the base case and variant case are quite similar.

Table 1. Channel Infiltration for Representative Years for Present-Day 90th Percentile Base-Case and Variant-Case Realizations

Representative Year	Weight	Base-Case Infiltration (mm/yr)	Variant-Case Infiltration (mm/yr)	Base-Case Weighted Infiltration (mm/yr)	Variant-Case Weighted Infiltration (mm/yr)
1	0.001	3.6	563.7	0.00	0.56
2	0.002	6.8	395.0	0.01	0.79
3	0.007	13.2	176.7	0.09	1.24
4	0.02	5.5	107.7	0.11	2.15
5	0.07	1.0	62.8	0.07	4.40
6	0.18	0.4	143.1	0.07	25.76
7	0.18	0.3	49.2	0.06	8.85
8	0.18	0.2	25.3	0.03	4.55
9	0.18	0.1	0.3	0.01	0.06
10	0.18	0.1	14.6	0.02	2.63

For evaluation of damping of infiltration transients by the PTn unit, two one-dimensional model simulations with pulsed infiltration were used, with PTn thicknesses of 81 and 21 m (SNL 2007, Section 6.9, Figures 6.9-2 and 6.9-3). Episodic infiltration pulses at the rate of 10,080 mm/yr were applied to the model top boundary for one week every 50 years, for 2,000 years. For the non-pulse infiltration period, a background infiltration rate of 28.1 mm/yr was applied. Together these functions produce a long-term average infiltration rate of 32 mm/yr. These simulations show that the PTn unit can attenuate such transients significantly. Discussion provided in the

response to RAI 3.2.2.1.2.1-5-005 explains that the resulting fluctuations in percolation flux at the repository horizon are encompassed by the uncertainty of infiltration as represented in the total system performance assessment model, and that repository performance is similar for the pulsed infiltration and the non-pulsed infiltration cases. Accordingly, temporal variability resulting from transient, focused infiltration in channels (at the expense of distributed infiltration elsewhere over the repository footprint) with a magnitude similar to transients previously evaluated, is not significant to repository performance.

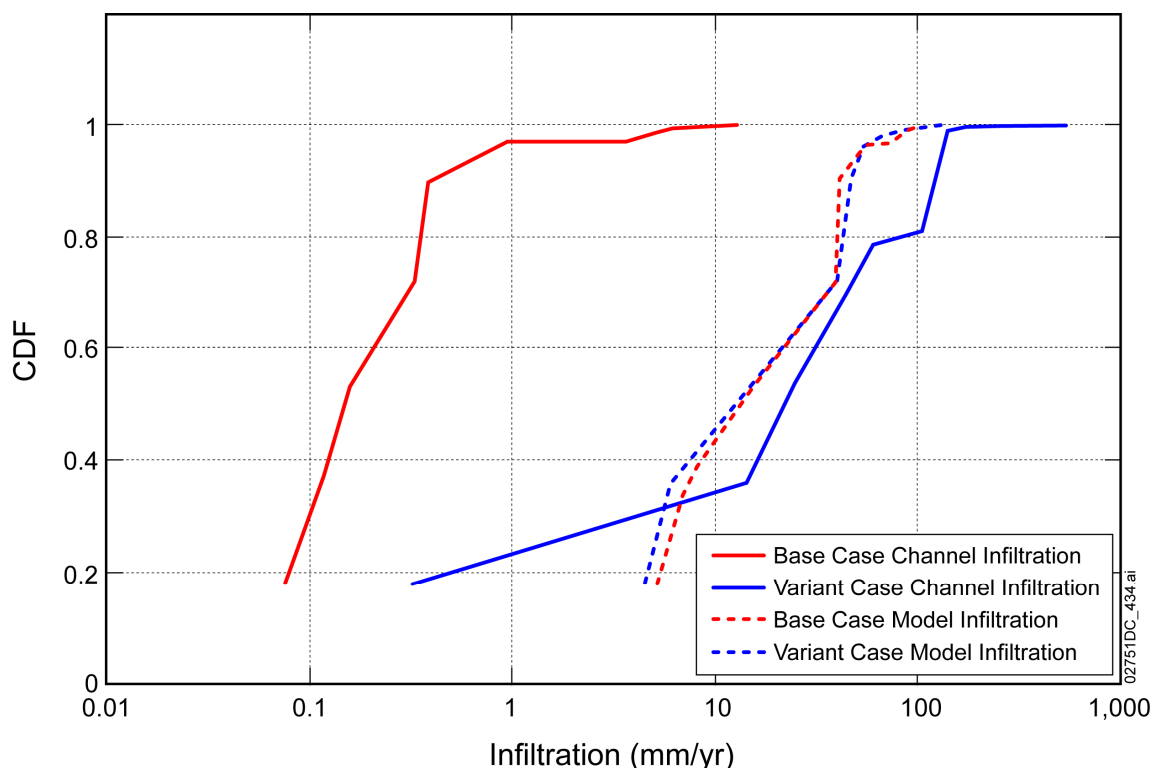


Figure 1. Cumulative Distribution Functions for Present-Day 90th Percentile Base-Case and Variant-Case Temporal Channel Infiltration, and Average Infiltration over the MASSIF Model Domain, Resulting from Temporal Variability in Annual Precipitation

Figure 2 shows the resulting stochastic simulations of channel infiltration for the base case and the variant case for 1,000 years, plotted with the transient infiltration condition used for the damping studies. Although the MAI for the variant case (51 mm/yr) is greater than that for the damping study (32 mm/yr) overall, annual averages of channel infiltration in the variant case exceed the background level for the damping study (28.1 mm/yr) only 52% of the time, and exceed the magnitude of transient pulses from the damping study only about 0.3% of the time. The distribution of the variant-case infiltration nearly evenly above and below the background infiltration for the PTn damping study indicates that the results are comparable, and the conclusions of the previous study apply (SNL 2007, Section 6.9). Figure 2 also shows that the frequency of relatively high pulses of infiltration for the variant case is greater than the 50-year pulse frequency for the PTn damping study, but that the magnitude is usually about half that of the PTn damping study. The frequency and magnitude of the variant-case pulses are therefore

closer to steady-state, and the transient damping demonstrated for the PTn damping study also applies to the variant case. Therefore, locally damp conditions in the PTn are not expected under the PTn damping study scenario or the variant-case scenario.

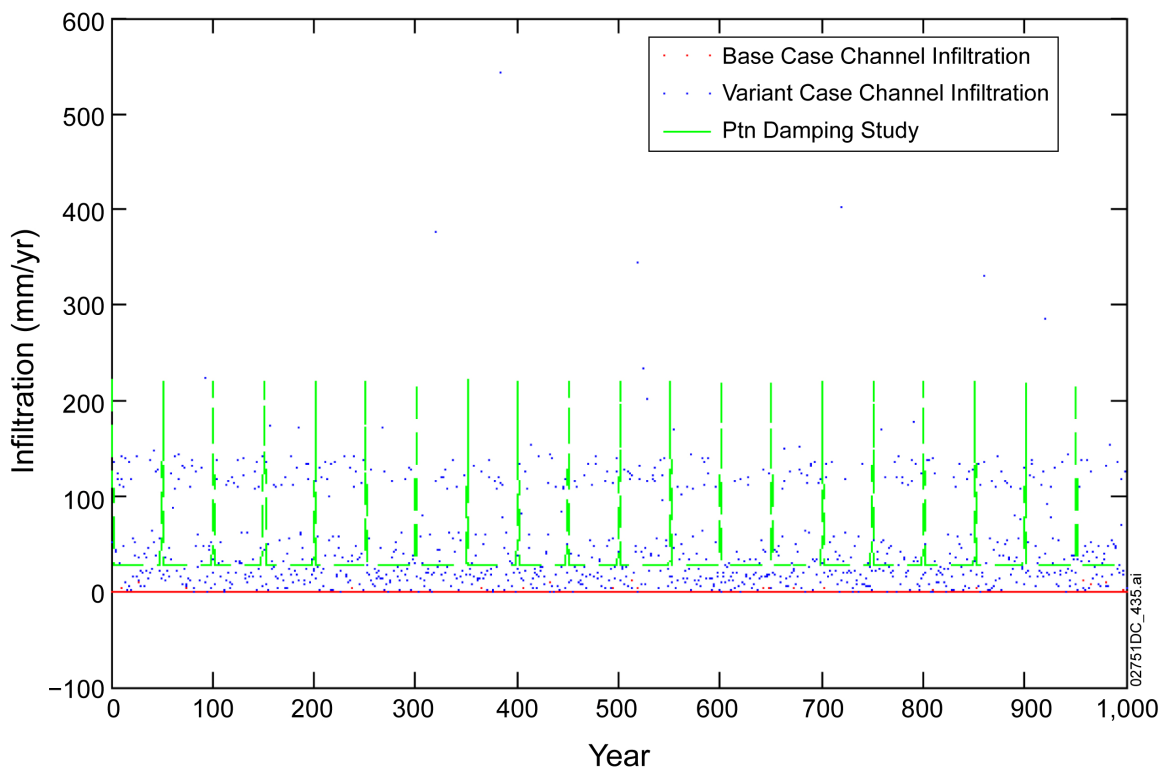


Figure 2. Present-Day 90th Percentile Base-Case and Variant-Case Channel Infiltration, and the Infiltration Boundary Condition for the PTn Damping Evaluation, for 1,000 Years

### 1.3.2 Spatial Damping of Channel Infiltration

Figure 3 presents CDFs showing the spatial variability of mean annual net infiltration, for the base-case and variant-case infiltration, for the present-day 10th and 90th percentile realizations, and shows that the base case and variant case are quite similar. The base-case and variant-case results for the 10th percentile realizations appear different for MAI of less than about 0.1 mm/yr because the variant-case results have many more grid cells with net infiltration rates of zero (in highland areas), and the x-axis of Figure 3 has a log scale in which zero values cannot be plotted.

The response to RAI 3.2.2.1.3.6-006 evaluated the sensitivity of repository performance to the flow focusing factor distribution used to represent intermediate-scale focusing behavior in the unsaturated zone. The response concluded that repository performance is not sensitive to spatial variability in seepage, and that radionuclide releases from the engineered barrier system are adequately estimated using spatially averaged seepage rates. Because spatially averaged infiltration is similar in the base case and the variant case, seepage rates and the resulting

estimates of repository performance are also similar. Consequently, estimates of repository performance are not sensitive to spatial variability in mean annual net infiltration.

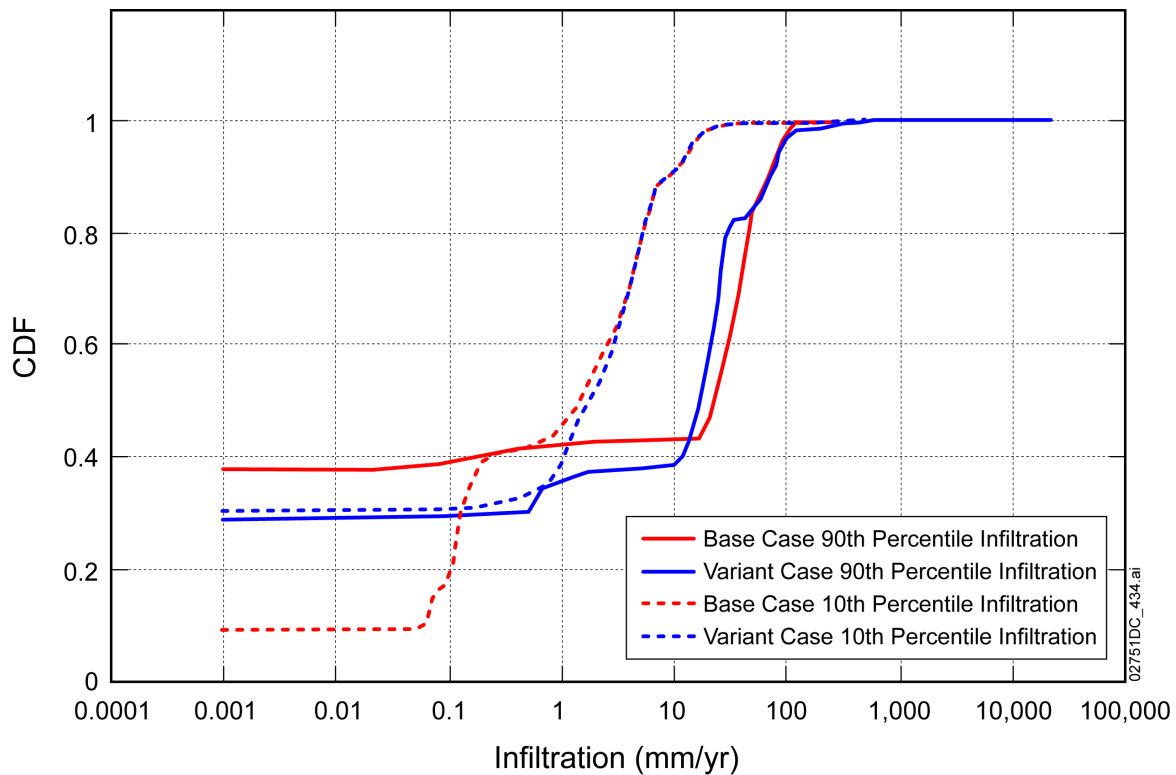


Figure 3. Cumulative Distribution Functions for Spatial Variability in Mean Annual Net Infiltration for Present-Day 10th and 90th Percentile Base-Case and Variant-Case over the MASSIF Model Domain

#### 1.4 SUMMARY

Channel infiltration as simulated using the variant case is not representative of repository conditions because of the changes made to soil and bedrock properties. The variant case produces increased runoff and channel infiltration (i.e., more focused infiltration) compared to the base case (more distributed infiltration). However, spatially averaged MAI is similar between these two cases, for scales extending from the entire model domain to the area of Pagany Wash, because in the variant case runoff readily infiltrates in the channels.

The consequences of more focused infiltration as represented by the variant case are insignificant to repository performance, and repository performance is therefore not overestimated. This is demonstrated by two previous analyses that considered temporal damping of transient infiltration in the PTn layer (SNL 2007, Section 6.9), and the sensitivity of repository performance to spatial variability in seepage (see response to RAI 3.2.2.1.3.6-006).

## 2. COMMITMENTS TO NRC

None.

## 3. DESCRIPTION OF PROPOSED LA CHANGE

None.

## 4. REFERENCES

LeCain, G.D.; Lu, N.; and Kurzmack, M. 2002. *Use of Temperature, Pressure, and Water Potential Data to Estimate Infiltration and Monitor Percolation in Pagany Wash Associated with the Winter of 1997–98 El Niño Precipitation, Yucca Mountain, Nevada*. Water Resources Investigations Report 02-4035. Denver, Colorado: U.S. Geological Survey.  
ACC: MOL.20020925.0158.<sup>a</sup>

SNL (Sandia National Laboratories) 2006. *Data Analysis for Infiltration Modeling: Extracted Weather Station Data Used to Represent Present-Day and Potential Future Climate Conditions in the Vicinity of Yucca Mountain*. ANL-MGR-MD-000015 REV 00. Las Vegas, Nevada: Sandia National Laboratories. ACC: DOC.20070109.0002; DOC.20070208.0009.

SNL 2007. *UZ Flow Models and Submodels*. MDL-NBS-HS-000006 REV 03 AD 01. Las Vegas, Nevada: Sandia National Laboratories. ACC: DOC.20080108.0003; DOC.20080114.0001; LLR.20080414.0007; LLR.20080414.0033; LLR.20080522.0086; DOC.20090330.0026<sup>b</sup>.

SNL 2008. *Simulation of Net Infiltration for Present-Day and Potential Future Climates*. MDL-NBS-HS-000023 REV 01 AD 01. Las Vegas, Nevada: Sandia National Laboratories. ACC: DOC.20080201.0002; LLR.20080507.0008; LLR.20080522.0101.

NOTES: <sup>a</sup>Provided as an enclosure to letter from Williams to Sulima, dtd 6/5/09, “Yucca Mountain – Request for Additional Information – Volume 3, Chapter 2.2.1.2.1, 5th Set (Scenario Analysis) (Department of Energy’s Safety Analysis Report Section 2.2, Table 2.2-5).”

<sup>b</sup>Provided as an enclosure to letter from Williams to Sulima dtd 6/01/09, “Yucca Mountain – Request for Additional Information – Safety Evaluation Report, Volume 3 – Postclosure Chapter 2.2.1.3.6 – Flow Paths in the Unsaturated Zone, Set 1 – (Department of Energy’s Safety Analysis Report Sections 2.3.2 and 2.3.3).”

**RAI Volume 3, Chapter 2.2.1.3.5, First Set, Number 7:**

Clarify why the number of soil depth observations used to represent the range and distribution of soil depth in each soil depth class across YM is appropriate such that net infiltration is not underestimated. Of particular concern are areas with soil depth less than 0.5 m. This information is needed to evaluate compliance with 10 CFR 63.114(a)(1,2).

Basis: A small number of observations from a portion of the geomorphic environments across YM is used to support the spatially variable and uncertain parameterization of soil depth in the infiltration model.

The focus on observations in support of DOE's estimates for Soil Depth Class 4 (0.1 to 0.5 m) is based on the sensitivity and nonlinearity of net infiltration results in general to soil depth, but also the sensitivity and nonlinearity within the range of values comprising Soil Depth Class 4. The latter refers to the choice of a uniform distribution for sampling soil depth in the 0.1 to 0.5 m range of Soil Depth Class 4, and the effect of that choice on infiltration results. Soil Depth Class 4 subsumes the majority (>70%) of the infiltration model, UZ flow model, and repository footprint domains and is represented by 35 soil depth samples.

**1. RESPONSE**

The representation of soil depth does not lead to underestimating infiltration. This response explains the methodology used to represent uncertainty in spatial variability distribution for soil depth (using upper and lower bound distributions) and, from the resulting distributions, uncertainty in the upscaled soil depth values.

**1.1 CONCEPTUAL DESCRIPTION OF THE DISTRIBUTION OF UNCERTAINTY**

The infiltration model area is divided into five soil depth classes. Each of the first four soil depth class regions is associated with a spatial distribution of soil depth. The fifth soil depth class represents bare rock (soil depth = 0 m), and therefore there is no uncertainty in this value. The other representations of the soil depth data for the other soil depth classes demonstrates that they are appropriately constrained and of less significance than Soil Depth Class 4 to estimates of infiltration.

Soil Depth Class 1 represents very thick soils, described by a uniform distribution with lower and upper bound values of 40 and 150 m, respectively. In deeper soils, infiltration is less likely to occur because deeper soil has a greater water holding capacity. The value chosen within this range is unlikely to cause a significant change to predicted infiltration (SNL 2008, Section 6.5.2.4[a]).

Soil Depth Class 2 represents moderately deep soils that range in depth from 0.5 to about 50 m. This class includes the value where soil depth is sufficient to limit infiltration of water to the soil-bedrock contact, except in some channels, because the soils have sufficient storage capacity

to retain precipitation in the root zone where it is subject to evapotranspiration. It is expected that infiltration is most likely to occur where soil thickness is small. Consequently, a reasonable value would lie closer to the small soil thickness portion of the distribution, rather than near the large soil thickness values (SNL 2008, Section 6.5.2.4[a]).

Soil Depth Class 3 represents areas of foot-slope soils that occur intermittently in the area. The data are represented by a log-normal distribution with an estimated population mean soil depth of 3.25 m and a sample median of 2.07 m, which is also the estimated population median; only one value is larger than 5.18 m (BSC 2006, Figure 6-15 and Table 6-7). As seen in Figure 6.5.2.4-1[a] of *Simulation of Net Infiltration for Present-Day and Potential Future Climates* (SNL 2008), Soil Depth Class 3 is most often found between soils of Soil Depth Class 2 (moderately deep) and Soil Depth Class 4 (shallow), acting as a transition from deeper to shallower soils. The depth in Soil Depth Class 3 is small where it contacts Soil Depth Class 4 but increases where it contacts deeper depth classes, primarily Soil Depth Class 2. The majority of infiltration through Soil Depth Class 3 will occur where the depth is small. There are 15 measurements for this depth class, four of which indicate that there is no soil. Although it is common to choose the median of a log-normal distribution as a measure of central tendency, because many of the samples were from disturbed sites that may underestimate soil depth, the greater sample mean of 3.26 m is a better measure of central tendency than the median in this case. The 90% confidence interval about the mean ranges from 2 to 7 m; the lower bound of this range is approximately the median (SNL 2008, Section 6.5.2.4[a]).

Soil Depth Class 5 represents exposed bedrock in the area that does not have soil cover. Therefore, all cells in this class are assigned a zero soil depth value (SNL 2008, Section 6.5.2.4[a]).

As shown in Figure 6.5.2.4-1[a] of *Simulation of Net Infiltration for Present-Day and Potential Future Climates* (SNL 2008, Section 6.5.2.4[a]), Soil Depth Class 4 encompasses the majority of the infiltration model domain. Soil Depth Class 4 represents the shallowest soils in the infiltration model domain and covers 71% of the unsaturated zone model domain and 57% of the infiltration model domain (SNL 2008, Table 6.5.2.4-1[a]). A single, upscaled value of soil depth was sampled uniformly, once per realization, from the uncertainty distribution and applied to every model node in Soil Depth Class 4. This value is called an upscaled quantity, as it was scaled from spatially variable soil depth data (on the order of a square meter on the surface) to a single value for the entire area of Soil Depth Class 4 (71 km<sup>2</sup>).

The methodology used to constrain the stochastic representation of Soil Depth Class 4 consists of:

- Construction of several spatial variability distributions for Soil Depth Class 4
- Selection of an upscaled quantity to be used from the distribution
- Estimation of the uncertainty in this upscaled quantity
- Demonstration that the upscaled quantity does not underestimate net infiltration.

### 1.1.1 Construction of Spatial Variability Distributions for Soil Depth Class 4

The soil depth data for Soil Depth Class 4 originally consisted of 35 measurements made on site (BSC 2006; SNL 2008, Figure 6.5.2.4-3[a]). The 35 measurements for Soil Depth Class 4 were sorted by depth, and each measurement was assigned a weight of 1/35. The spatially variable data were then fitted to a log-normal distribution. Two methods of fitting were considered: (1) probability plot fit and (2) least squares fit (SNL 2008, Figure 6.5.2.4-3[a]). Although some areas within the region of Soil Depth Class 4 do consist of bare rock, none of the data reported in the 35 measurements were equal to zero, which corresponds to bare rock. This may indicate a bias towards deeper soils.

Used as a source of corroborating data, soil depths were measured by the Center for Nuclear Waste Regulatory Analyses (CNWRA) during two site visits to Yucca Mountain (Fedors 2007). Maximum and minimum soil depths were recorded for many locations. Slope of the bedrock surface was also approximated. A total of 56 values of representative soil depth were recorded. The 56 values of representative soil depth collected by the CNWRA (Fedors 2007) were compared to the original soil depth data set consisting of 35 soil depth measurements (BSC 2006) that was used to characterize shallow Soil Depth Class 4 (SNL 2008, Section 7.2.4[a]).

Statistical analysis of the CNWRA data and the 35 soil depth measurements indicates that the CNWRA samples are slightly shallower than the 35 soil depth measurements, based on their mean, median, and geometric mean values. A summary of the statistical analysis is shown in Table 7.2.4-1[a] of *Simulation of Net Infiltration for Present-Day and Potential Future Climates* (SNL 2008). The CNWRA data set, like the 35 soil depth measurements, was found to have a log-normal distribution. Results of a Wilcoxon rank-sum test comparing these two data sets for similarity of distribution (and not similarity of mean) show that the hypothesis of similarity of distributions can be rejected (SNL 2008, Section 7.4.2[a]). This supports the fact that the 35 measurements define an optimistic spatial variability distribution, in the sense that deeper soils lead to lower net infiltration.

As the distribution for the 35 measurements was considered optimistic, another source of information was used to create a second spatial distribution of shallow soil depth which documented eight more observations based on photographs of soil in the area. These additional eight observed soil depth ranges are tabulated in Table 6.5.2.4-4[a] of *Simulation of Net Infiltration for Present-Day and Potential Future Climates* (SNL 2008). This second distribution was constructed using a Monte Carlo approach (SNL 2008, Figure 6.5.2.4-4[a]) to represent the piecewise distribution.

The two fitting methods mentioned above (probability plotting and least squares) were also applied to the eight observed soil depth ranges. Because 25% of the distribution is equal to zero and a log-normal distribution is not defined for values of zero, each of these fitting methods had to be modified. Two approaches were utilized in modifying the fitting methods (SNL 2008, Section 6.5.2.4.1[a]):

- The first approach assumed that the information available is known only for values greater than zero and that nonzero values represent only 75% of the distribution. This assumption allows calculation of the arithmetic and geometric means of the fitted log-normal distributions directly, but it tends to over-represent the shallow soils and is therefore conservative.
- The second approach assumed that the distribution is bimodal. Like the first approach, the fitting was done with nonzero values; however, they were considered to represent the whole distribution. The final estimates of the arithmetic and geometric means were corrected to include 25% of zero values. This approach led to a better fit, but it required making these assumptions to calculate a meaningful geometric mean.

Spatial variability is thus represented by three distributions: a log-normal distribution based upon 35 on-site measurements (an upper bound, giving larger values of soil depth resulting in lower values for infiltration) and two based on eight on-site observations and photography using the two approaches discussed above. The first is the 75% log-normal distribution which is considered a lower bound, giving smaller values of soil depth (resulting in higher values for infiltration) (SNL 2008, Figure 6.5.2.4-6[a]). The second is the bimodal distribution, which is considered the intermediate, and it provides a closer fit to the data set of 35 measurements. These are used to generate site wide soil depth values that encompass both spatial variability and uncertainty of the values.

### **1.1.2 Selection of the Upscaled Quantity**

Because of nonlinearities between soil depth and average net infiltration, it is not expected that either single statistic would best represent an effective uniform value of soil depth leading to an accurate estimate of spatially averaged net infiltration.

In hydrologic modeling, flow parameters such as permeability (typically represented with a log-normal spatial distribution) are generally upscaled to the geometric mean, and storage parameters such as porosity (typically represented with a normal spatial distribution) are typically upscaled to the arithmetic mean. Soil depth follows a log-normal spatial distribution but is a storage-type parameter. Therefore, the upscaled value should lie between the geometric and arithmetic means (SNL 2008, Section 6.5.2.4.1[a]).

Both the geometric mean and the arithmetic mean are therefore considered equally probable. Both have been estimated for the fitted log-normal distributions and results are displayed for the geometric mean in Table 6.5.2.4-5[a] and for the arithmetic mean in Table 6.5.2.4-6[a] of *Simulation of Net Infiltration for Present-Day and Potential Future Climates* (SNL 2008).

### 1.1.3 Estimation of the Uncertainty in the Upscaled Quantity

Three distributions were considered. Each distribution was fitted using two fitting methods: (1) least squares fit; and (2) probability plot fit. This provided six ways to estimate the upscaled quantity. As two upscaled quantities were considered (one from the geometric mean and one from the arithmetic mean), this provided 12 estimates for the representative value (see schematic in Figure 1). For each, a lower bound and an upper bound was estimated by adding or subtracting one standard error to the value (capturing the uncertainty due to the small number of photographs or measurements available in each case), which represents that value's confidence interval. The minimum and maximum values of the bounds represent the uncertainty in the upscaled quantity (SNL 2008, Tables 6.5.2.4-5[a] and 6.5.2.4-6[a]).

If any of the values of a distribution are equal to zero, the geometric mean is equal to zero. Thus, the inclusion of zero values will lead to a useless estimate. One solution is to associate a very small (constant) value to represent the fraction of the spatial distribution with zero soil depth. As the geometric mean is equivalent to an arithmetic mean calculated on log-transformed data, taking a value too small will lead again to a very low value of the geometric mean. Therefore, the presence of 1 cm of soil is essentially equivalent to no soil regarding the resulting net infiltration. The geometric mean was then estimated using log-transformed data, estimating the mean and its confidence bounds, summing 75% of these bounds with 25% of the logarithm of 0.01 m (approximately  $-4.6$ ), and exponentiating the results to convert to a linear scale. Higher values of soil depth, from 2 to 9 cm, have been tested to represent the fraction of bare rock and to estimate the sensitivity of confidence bounds to the selected values. With 10-cm accuracy, all values result in the same confidence interval (SNL 2008, Section 6.5.2.4[a], p. 6-46).

The minimum value estimate is thus set equal to 0.1 m (bounds for the geometric mean using the probability plot fitting method on the second data set using the first approach, and for the geometric mean on the second data set using the second approach). The maximum is equal to 0.5 m (upper bound of the arithmetic mean using the probability-plot fitting method on the first data set). Because there is no reason to favor any of these values (or any intermediate value), a uniform distribution for soil depths between 0.1 and 0.5 m was selected to represent the uncertainty in the upscaled quantity used to represent the effective uniform value of Soil Depth Class 4 (SNL 2008, Tables 6.5.2.4-5[a] and 6.5.2.4-6[a]).

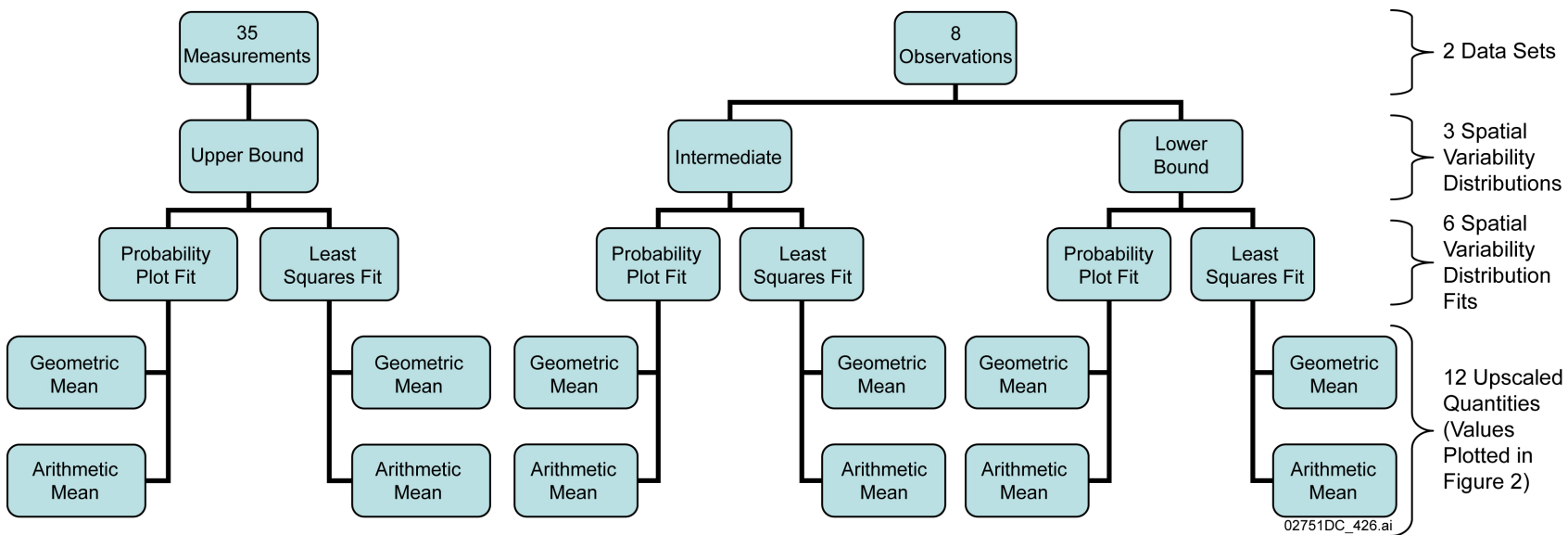


Figure 1. Schematic Showing How the Uncertainty Distribution for the Upscaled Quantity of Soil Depth Is Developed

**1.1.4 Demonstration That a Uniform Distribution Is Reasonable**

Section 6.5.2.4.1[a] of *Simulation of Net Infiltration for Present-Day and Potential Future Climates* (SNL 2008) discusses why a uniform distribution was selected for the uncertainty analysis rather than a log-normal distribution. It is important to note that the uniform distribution and the range selected represent the uncertainty in an upscaled quantity and not the spatial variability at every point of the domain. If the spatial variability of Soil Depth Class 4 was modeled by Mass Accounting System for Soil Infiltration and Flow (MASSIF) by taking a different value for Soil Depth Class 4 at each corresponding cell in the domain, then a log-normal distribution would have been used. Since one value for Soil Depth Class 4 is used for a given realization by MASSIF, this value cannot represent the spatial variability distribution. This upscaled value is expected to lie between the median and arithmetic mean, which is why a range of 0.1 to 0.5 m was selected (SNL 2008, Section 6.5.2.4.1[a]). If a log-normal distribution was used with the full range of Soil Depth Class 4 (0 to 3 m) for the Latin Hypercube Sampling (LHS) of soil depth, then deeper soil depths would be sampled than using a uniform distribution for a range of soil depths between 0.1 and 0.5 m. The reason for using a uniform distribution for the ranges described above is that there is not enough information suggesting how to weight the values between the median and the mean.

The twelve estimates of the mean reported in Tables 6.5.2.4-5 and 6.5.2.4-6 of *Simulation of Net Infiltration for Present-Day and Potential Future Climates* (SNL 2008) are sorted after modifying the fitting methods as discussed in Section 1.1.1, and plotted as a cumulative distribution function in Figure 2. The resulting relationship is quite similar to a uniform distribution between approximately 0.1 m and 0.5 m. A uniform distribution would give an  $R^2 = 1.0$ , while here it is  $R^2 \sim 0.99$ . Therefore, the use of a uniform distribution to represent the upscaled quantity of soil depth is reasonable.

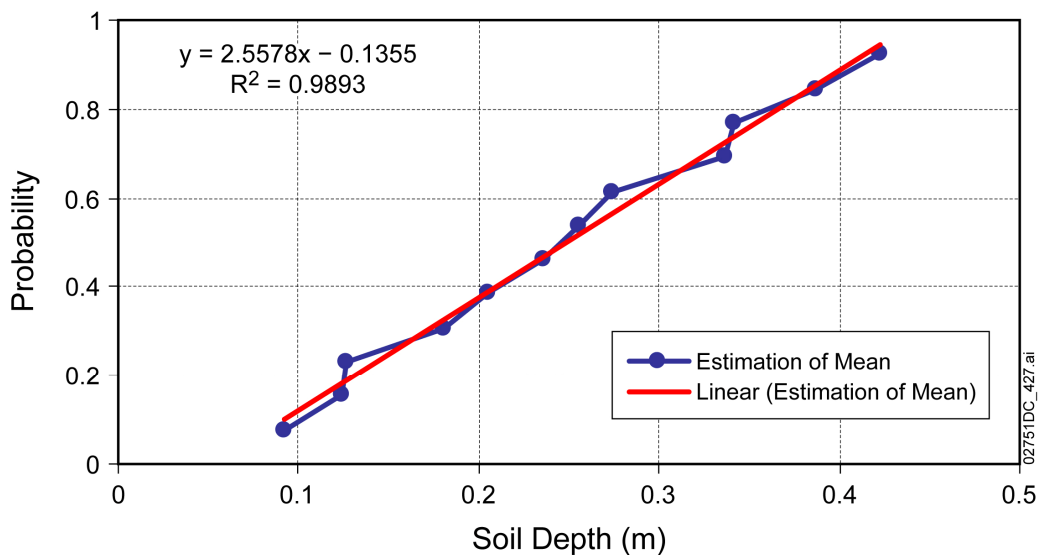


Figure 2. Cumulative Distribution Function of the Estimates of the Arithmetic Mean and Geometric Mean Soil Depths

### 1.1.5 Demonstration That Net Infiltration Is Not Underestimated

The relationship between Soil Depth Class 4 and average net infiltration is discussed in the sensitivity analysis presented in Appendix H of *Simulation of Net Infiltration for Present-Day and Potential Future Climates* (SNL 2008). Two types of sensitivity analyses are considered. The first evaluates the overall influence of all the uncertain parameters on the variance of the net average infiltration without distinction between aleatory and epistemic uncertainty. The second focuses on physical parameters by fixing a representative value to the aleatory uncertain parameters (i.e., due to randomness of future conditions).

In both analyses, Soil Depth Class 4 is a major contributor of the net infiltration variance, being the most important physical parameter and of equal importance as uncertainty in precipitation. Scatterplots of average infiltration vs. Soil Depth Class 4 (SNL 2008, Figures H1 to H9) show a generally linear behavior with a linear effect of the uncertainty in Soil Depth Class 4 on the uncertainty in net infiltration. It is important to note that for Figures H3 and H4 of *Simulation of Net Infiltration for Present-Day and Potential Future Climates* (SNL 2008), the apparent super-linear relation for shallow soil is due to the fact that low values of soil depth are associated with low values of holding capacity. The holding capacity is the second most important physical parameter in terms of the sensitivity analysis and has a negative linear relationship with net infiltration.

The uncertainty in Soil Depth Class 4 has been characterized such that it was neither optimistic nor pessimistic and that shallow depths were not underrepresented. The linear relation between the uncertainty in Soil Depth Class 4 and in net infiltration allows transposing this conclusion to net infiltration. Therefore, the distribution of net infiltration is not underestimated.

### 1.1.6 Summary

Soil Depth Class 4 encompasses the majority of the infiltration model domain and spatial variability distributions were developed for this soil depth class. Optimistic (upper bound, deeper soil, low infiltration) and pessimistic (lower bound, shallow soil, high infiltration) distributions were developed: one optimistic distribution based on 35 soil depth measurements and two pessimistic distributions based on 8 photographic observations in the Yucca Mountain area. The spatially variable data were fitted using two methods: (1) probability plot fit and (2) least squares fit, leading to six fitted spatially variable distributions. From each fitted distribution, a geometric mean and arithmetic mean were estimated, leading to twelve estimates of the upscaled quantity of soil depth. A uniform distribution for soil depths between 0.1 and 0.5 m was selected to represent the uncertainty in the upscaled quantity used to represent the effective uniform value of Soil Depth Class 4. The twelve estimates of the mean were sorted and plotted as a cumulative distribution function, which proved that the use of a uniform distribution to represent the upscaled quantity of soil depth is reasonable.

Two types of sensitivity analyses were considered for the relationship between soil depth and net infiltration. In both analyses, Soil Depth Class 4 was a major contributor of the net infiltration variance, being the most important physical parameter. Scatterplots of average infiltration vs. Soil Depth Class 4 showed a linear effect of the uncertainty in Soil Depth Class 4 on the

uncertainty in net infiltration. The linear relation between the uncertainty in Soil Depth Class 4 and in net infiltration allows transposing this conclusion to net infiltration. Therefore, the distribution of net infiltration is not underestimated.

## **2. COMMITMENTS TO NRC**

None.

## **3. DESCRIPTION OF PROPOSED LA CHANGE**

None.

## **4. REFERENCES**

BSC (Bechtel SAIC Company) 2006. *Data Analysis for Infiltration Modeling: Technical Evaluation of Previous Soil Depth Estimation Methods and Development of Alternate Parameter Values*. ANL-NBS-HS-000077 REV 01. Las Vegas, Nevada: Bechtel SAIC Company. ACC: DOC.20060918.0009.

Fedors, R. 2007. "Soil Depths Measured at Yucca Mountain During Site Visits in 1998." Letter from R. Fedors to J. Guttman, January 9, 2007. ACC: LLR.20070815.0081.

SNL (Sandia National Laboratories) 2008. *Simulation of Net Infiltration for Present-Day and Potential Future Climates*. MDL-NBS-HS-000023 REV 01 AD 01. Las Vegas, Nevada: Sandia National Laboratories. ACC: DOC.20080201.0002; LLR.20080507.0008.

**RAI Volume 3, Chapter 2.2.1.3.5, First Set, Number 8:**

Explain why the use of a pedotransfer function to estimate spatially distributed soil hydraulic properties, in combination with lumping together soil groups 5, 7, and 9, does not lead to underestimates of net infiltration in the next 10,000 years. This information is needed to evaluate compliance with 10 CFR 63.114(a)(1,2).

Basis: Uncertainty in parameterization of spatially variable and highly nonlinear soil hydraulic properties can lead to uncertainty in estimating net infiltration. Depending on the application, pedotransfer functions often do not perform well in predicting soil hydraulic properties, and may lead to underestimates of net infiltration because of an underestimate of soil hydraulic property variability (e.g., Wang, et al., 2009). Instead of using site-specific data for soil hydraulic properties, DOE uses a pedotransfer function developed from soils at Hanford to estimate hydraulic properties for YM soils. The spatial variability may be further reduced by the use of a soil class that is a combination of a combination of soil groups 5, 7, and 9. As a model input, this soil type appears to cover >95 percent of the repository footprint (visual estimate from SAR Figure 2.3.1-18).

**1. RESPONSE****1.1 BACKGROUND**

Estimates of soil properties using a pedotransfer function (PTF) have been compared with both site-specific and regional soil data to demonstrate the PTF approach provides conservative values of net infiltration. The results of a comparison of MASSIF model results using MASSIF, site-specific, and regional soil properties demonstrate net infiltration is not underestimated.

The MASSIF infiltration model (SNL 2008) is a field-capacity model, also known as a “bucket model.” The basis for the bucket model is that water moves downward from one soil layer to the next only if the soil water content of the overlying layer exceeds its field capacity. The MASSIF model uses a default value of field capacity defined as the average of the soil water content at soil water potentials of  $-0.1$  and  $-0.33$  bars. The rationale for this selection is provided in *Simulation of Net Infiltration for Present-Day and Potential Future Climates* (SNL 2008, Section 6.5.2.3) and in *Data Analysis for Infiltration Modeling: Development of Soil Units and Associated Hydraulic Parameter Values* (BSC 2006, Section 5.4; hereafter referred to as “the soils report”).

Soil hydraulic properties used in the MASSIF model were developed by matching the soil texture (percentages of sand, silt, and clay) of Yucca Mountain soil samples to the soil texture of samples cataloged in a soils database from the Hanford site (Khaleel and Freeman 1995). Soil hydraulic properties have been measured on site-specific Yucca Mountain soil samples (e.g., BSC 2004 and Guertal et al. 1994) and are compared to those developed for use in the MASSIF model.

The methodology used to estimate the hydraulic properties for the eight of the nine soil units that are used with the MASSIF model is documented in *Data Analysis for Infiltration Modeling: Development of Soil Units and Associated Hydraulic Parameter Values* (BSC 2006). One of the nine soil units is defined as bare rock (no soil cover), so only eight soil units are discussed here. Table 6-7 of the soils report (BSC 2006) provides the hydraulic properties of the eight soil units, including field capacities at water potential values of  $-0.1$  and  $-0.33$  bars, while Table 6-11 of the soils report (BSC 2006) provides the same properties but for lumped soil groups 1, 2/6, 3/4, and 5/7/9. The justifications and rationale for the lumping of soil groups is provided in Section 6.3.4.1 of the soils report (BSC 2006).

## 1.2 WATER HOLDING CAPACITY

Although soil wilting point, water holding capacity (WHC), porosity, and  $K_{sat}$  parameters are inputs to the MASSIF model, WHC is the most important of these because MASSIF is a field-capacity type model, where no downward flow can occur if the amount of water in a soil layer does not exceed the WHC, defined as field capacity minus soil wilting point (or the residual water content). The importance of WHC is confirmed by two sensitivity analyses discussed in SAR Section 2.3.1.3.3.2.2 and has been documented in detail (SNL 2008, Sections 6.7.2 and 7.1.4). Both analyses conclude that the two most sensitive parameters in the MASSIF model (excluding precipitation) are the soil depth for Soil Depth Class 4, and the WHC of soil group 5/7/9. When aleatory uncertainty is fixed, these two parameters account for 90% of the variance in mean net infiltration for present-day and glacial-transition climates, and for 75% of the variance for the monsoon climate (SNL 2008, Section 6.7.2). In the extended sensitivity analysis (conducted with 200 realizations, 42 uncertain parameters, a single present-day precipitation file, and a model domain consisting of Drill Hole Wash), approximately 80% of the variance in mean net infiltration was attributed to these same two parameters (SNL 2008, Section 7.1.4). The sensitivity of net infiltration to WHC is negative, meaning that lower values of WHC result in higher rates of net infiltration.

Given the importance of the WHC of soil group 5/7/9, it can be determined whether net infiltration is underestimated (as a result of the PTF approach and soil grouping), by comparing the range of WHC of soil group 5/7/9 used in MASSIF to the WHC estimated for site-specific soil samples. In addition, WHC values used in MASSIF were compared with those measured for a regional soils database for Nye County soils (USDA 2006a; discussed in BSC 2006, Section 6.4.4). Although the Nye County soil samples are not directly from Yucca Mountain, they are also useful for comparison.

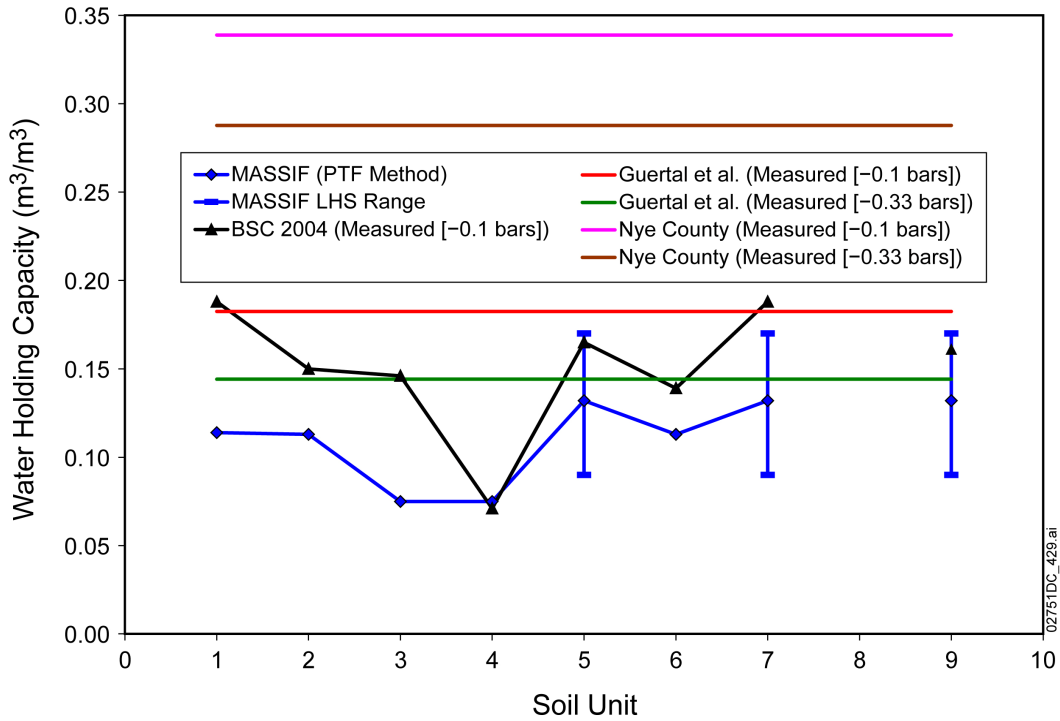
The MASSIF model generates 40 maps of net infiltration for each of the three future climates considered in the 10,000-year compliance period. For a given climate, each of these 40 maps provides an equally probable outcome of net infiltration over the modeling domain. The range of net infiltration values within the set of 40 maps provides a reasonable estimate of the uncertainty in magnitude of net infiltration. This uncertainty is estimated using the structured Monte Carlo technique of Latin Hypercube Sampling (LHS). This method propagates uncertainty in a collection of input parameters (such as WHC) to uncertainty in model outputs (net infiltration). The distribution of WHC for soil group 5/7/9 sampled during LHS was uniform—ranging from  $0.09$  to  $0.17$   $m^3/m^3$ . The minimum and maximum values of this range represent the mean WHC

of soil group 5/7/9 at water potentials of  $-0.33$  and  $-0.1$  bars, respectively (BSC 2006, Table 6-11). Figure 1 shows the mean WHC values for the MASSIF model, and the range of values used for the 5/7/9 group. Figure 1 also shows the WHC values used in a previous, less conservative version of the infiltration model (BSC 2004; hereafter referred to as the previous infiltration model), the mean of nine WHC values from one location near borehole UZ-N85 (Guertal et al. 1994), and the average WHC (at  $-0.1$  and  $-0.33$  bars) for the Nye County data set (USDA 2006a). Guertal et al. (1994) reported hydraulic properties that can be used to calculate field capacities at  $-0.1$  and  $-0.33$  bars. The Guertal et al. (1994) and Nye County (USDA 2006a) WHC values were both calculated using the average residual water content of  $0.035 \text{ m}^3/\text{m}^3$  from MASSIF (because residual water contents were not provided in these data sets).

Figure 1 shows that the MASSIF mean WHC values are: (1) less than the previous infiltration model (BSC 2004) values for seven of eight soil groups, (2) less than the Guertal et al. (1994) mean values, and (3) far less than the mean Nye County values.

Figure 2 compares the averages of these WHC values. The MASSIF 5/7/9 value of  $0.133 \text{ m}^3/\text{m}^3$  is the average of the WHC values at  $-0.1$  and  $-0.33$  bars for the 5/7/9 group from Table 6-11 of the soils report (BSC 2006). The “MASSIF 4 Groups” value of  $0.109 \text{ m}^3/\text{m}^3$  is the average of the WHC values at  $-0.1$  and  $-0.33$  bars of the four groups (1, 2/6, 3/4, and 5/7/9) from Table 6-11 of the soils report (BSC 2006). The previous infiltration model (BSC 2004) value of  $0.151 \text{ m}^3/\text{m}^3$  is the average value of WHC for eight soil units in Table B-4 of the previous infiltration report (BSC 2004), where WHC is water content at  $-0.1$  bars minus the water content at  $-60$  bars. The Nye County value of  $0.313 \text{ m}^3/\text{m}^3$  is the average of the Nye County field capacities shown in the soils report (BSC 2006, Figures 6-20 and 6-21), minus the average MASSIF residual water content.

The average values of WHC based on the PTF approach and soil grouping are lower than the site-specific and Nye County average WHC values. The lower end of the uncertainty distribution representing WHC based on the PTF approach is lower than all WHC measurements, with the exception of the previous infiltration report's (BSC 2004) measurement for Soil Unit 4 (Soil Unit 4 covers about 1% of the infiltration model domain). The negative relationship of net infiltration to WHC means that lower values of WHC result in higher rates of net infiltration, demonstrating that the WHC parameter values and uncertainty distributions based on the PTF approach do not lead to underestimates in net infiltration.



NOTE: The BSC 2004 field capacities are reported for a potential of -0.1 bars.

Figure 1. Comparison of MASSIF, Site-Specific, and Nye County WHC Values

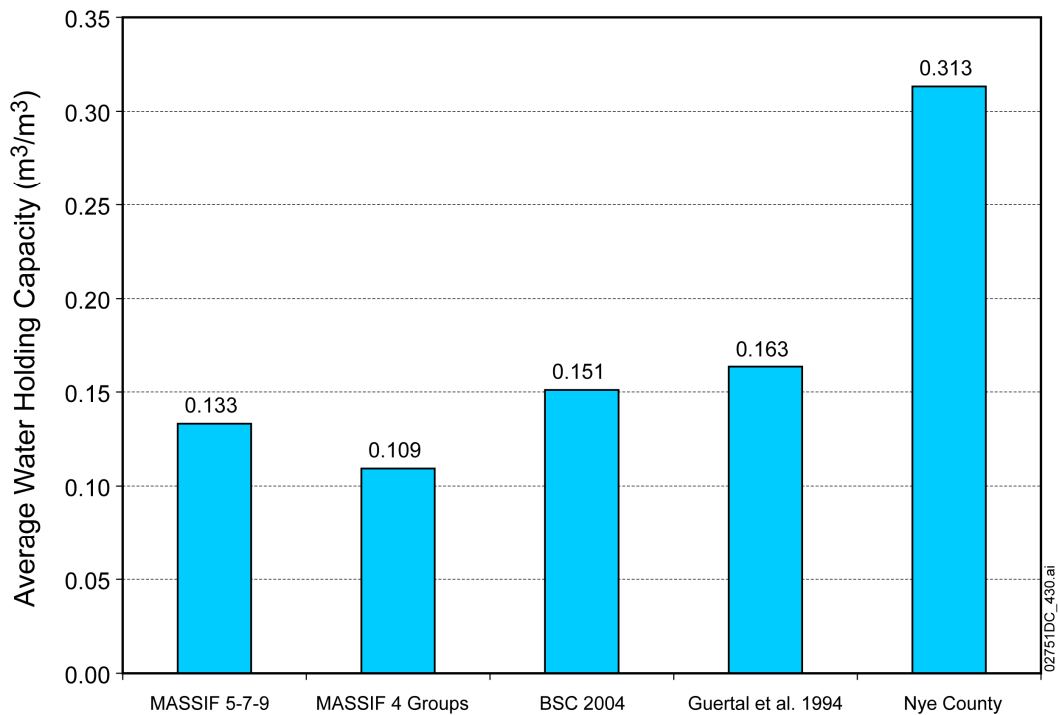


Figure 2. Comparison of Average MASSIF, Site-Specific, and Nye County WHC Values

### 1.3 SOIL SATURATED HYDRAULIC CONDUCTIVITY

Soil  $K_{sat}$  was also determined by the PTF approach. In general terms, if  $K_{sat}$  is underestimated, then more precipitated water will be diverted as runoff, at the expense of infiltration, and if  $K_{sat}$  is overestimated, then more precipitated water will infiltrate at the expense of runoff. However, this generalization depends on rainfall intensity. If rainfall intensity is low, then in general, net infiltration is insensitive to soil  $K_{sat}$ . If rainfall intensity is high, then net infiltration is more sensitive to soil  $K_{sat}$ . In the MASSIF model, runoff can occur if the rainfall intensity exceeds the soil  $K_{sat}$  or if the soil profile becomes completely saturated.

Figure 3 provides a comparison of soil  $K_{sat}$  values from the MASSIF model, the previous infiltration model (BSC 2004), Hofmann et al. (2000), Istok et al. (1994), and from the Nye County Soil Data Mart (USDA 2006b; discussed in BSC 2006, Section 6.4.7). The MASSIF model values include the upper and lower bounds of soil  $K_{sat}$  that were sampled as part of the extended sensitivity analysis (SNL 2008, Section 7.1.4). The Hofmann et al. (2000) values are from double-ring infiltrometer measurements conducted at two sites. The Istok et al. (1994) value is the geometric mean of the eight mean values reported in the soils report (BSC 2006, Table 6-19). These soil samples were collected at the Area 5 Radioactive Waste Management Site at the Nevada Test Site. The Nye County values' upper and lower bounds are described in the soils report (BSC 2006, Section 6.4.7) as representing "most soils" from this Nye County data set. As shown in Figure 3, MASSIF values of soil  $K_{sat}$  are considerably lower than site-specific and Nye County values.

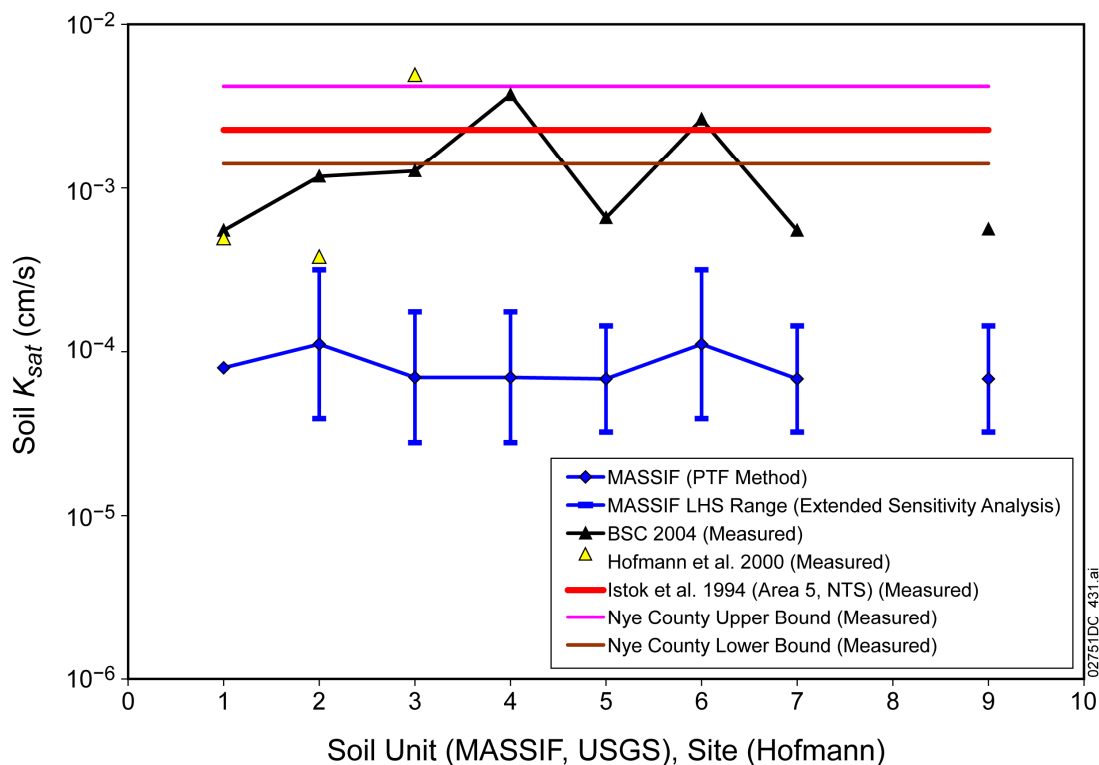


Figure 3. Comparison of Average MASSIF, Site-Specific, and Regional Soil  $K_{sat}$  Values

### 1.3.1 Sensitivity of Net Infiltration to Soil $K_{sat}$

In addition to its sensitivity to precipitation, MASSIF is primarily sensitive to soil depth in Soil Depth Class 4, and the WHC of soil group 5/7/9. In the extended sensitivity analysis (SNL 2008, Section 7.1.4), net infiltration was found to be largely insensitive to soil  $K_{sat}$ . Although soil  $K_{sat}$  for group 5/7/9 was more sensitive than many of the other 42 parameters sampled, soil  $K_{sat}$  for group 5/7/9 only accounted for about 1% of the variance in net infiltration in this analysis, with net infiltration increasing as group 5/7/9 soil  $K_{sat}$  increased (SNL 2008, Table 7.1.4-2). The reason for the insensitivity of net infiltration to soil  $K_{sat}$  is that rainfall intensity rarely exceeds soil  $K_{sat}$ . The climate state experiencing the greatest frequency of rainfall intensity exceeding soil  $K_{sat}$  is the monsoon climate.

### 1.3.2 Adjustments to Soil $K_{sat}$ s

SAR Section 2.3.1.3.4.1 and *Simulation of Net Infiltration for Present-Day and Potential Future Climates* (SNL 2008, Sections 7.1.3, 7.1.3.1, and 7.1.3.2[a]) describe the MASSIF model validation activities related to matching model results to streamflow and infiltration data. In the first activity (SNL 2008, Section 7.1.3), soil  $K_{sat}$  for all groups was decreased uniformly until MASSIF model streamflow output reasonably matched the streamflow data (see, for example, SAR Figure 2.3.1-46). In the second activity (SNL 2008, Section 7.1.3.1), soil  $K_{sat}$  was decreased for most soil groups, and increased for soil type 3 to be consistent with the results reported in *Simulation of Net Infiltration for Present-Day and Potential Future Climates* (SNL 2008, Section 7.2.1.1.2[a]) in which MASSIF  $K_{sat}$ s were adjusted to match reported infiltration at borehole UZ #4 (LeCain et al. 2002). In the third activity (SNL 2008, Section 7.1.3.2[a]), the adjustments described for the second activity (using the Pagany Wash variant property set) were applied to the entire MASSIF model domain.

The results of the first activity showed that soil  $K_{sat}$  had to be decreased, rather than increased (towards the site-specific  $K_{sat}$  values), in order to match streamflow data. The results of the second and third activities indicated that while the application of the Pagany Wash variant parameter set changed the spatial distribution of runoff versus infiltration, it had very little effect on the spatial averages of net infiltration, or the total runoff. Comparison of SAR Figure 2.3.1-27 with Figure 7.1.3.2-2[a] of *Simulation of Net Infiltration for Present-Day and Potential Future Climates* (SNL 2008) shows the present-day 30th percentile net infiltration maps for the base case and the variant soil  $K_{sat}$  case, respectively. In the base-case figure, infiltration is relatively higher in the highlands (areas dominated by thin soils and no channels), and relatively lower in the stream channels compared to the variant-case figure. Despite these differences in the spatial distribution of net infiltration, the average net infiltration and runoff results for the entire infiltration model domain, the unsaturated zone model domain, and the repository footprint are similar between the base case and variant cases (see SNL 2008, Table 7.1.3.2-1[a]).

The explanation for the need to decrease, rather than increase, soil  $K_{sat}$  to match streamflow data in the first activity is, in part, related to the large uncertainty in simulating rainfall duration. The MASSIF model applies a linear function, based on precipitation amount, to estimate rainfall duration. The relationships between rainfall duration and rainfall amount for the Yucca

Mountain and analogue climate sites are shown in *Simulation of Net Infiltration for Present-Day and Potential Future Climates* (SNL 2008, Figures 6.5.1.7-1[a] to 6.5.1.7-4[a]). There is a lack of correlation in these figures. An additional explanation is the effect of bedrock  $K_{sat}$  in combination with shallow soils. As discussed in SAR Section 2.3.1.3.2.1.4, the bedrock  $K_{sat}$  values used with MASSIF are probably biased toward overestimation. Because the bedrock and soil  $K_{sat}$ s used in MASSIF are about the same magnitude, bedrock does not act to slow down net infiltration (and cause runoff in cases of a completely saturated soil profile). Thus, the decrease in soil  $K_{sat}$  required to match streamflow data in the first activity may have effectively reduced bedrock  $K_{sat}$ s.

#### 1.4 COMPARISON OF SOIL PROPERTY SETS USING MASSIF

To demonstrate that the use of a PTF to estimate spatially distributed soil hydraulic properties, in combination with lumping together soil groups 5/7/9, does not lead to underestimates of net infiltration in the next 10,000 years, MASSIF model results were compared with those recalculated using the alternative soil properties discussed above.

For this comparison, the model scenario described in SAR Section 2.3.1.3.4.2.1 and in *Simulation of Net Infiltration for Present-Day and Potential Future Climates* (SNL 2008, Section 7.2.1.1.2[a]) was used for the Pagany Wash borehole UZ #4; first the Lower Pagany Wash (LPW) watershed, and then the much larger Drill Hole Wash (DHW) watershed for model domains, and weather data from the Site 3 station for water years 1994 to 1998 (five years). For soil properties, the MASSIF nominal values, the previous infiltration report (BSC 2004) model values, and the average Nye County values were used.

Figures 4 and 5 show the sorted infiltration results for every grid cell for LPW and DHW, respectively. The average infiltration for the LPW domain was 10.6, 9.8, and 7.2 mm/yr for the MASSIF, the previous infiltration report (BSC 2004), and Nye County soils, respectively. The average infiltration for the DHW domain was 6.0, 5.4, and 3.6 mm/yr for the MASSIF, the previous infiltration report (BSC 2004), and Nye County soils, respectively. For the LPW domain, average infiltration using MASSIF soil properties was 8.0% greater than when using properties from the previous infiltration report (BSC 2004), and 37.2% greater than when using Nye County soil properties. For the DHW domain, average infiltration using MASSIF soil properties was 12.5% greater than when using the previous infiltration report (BSC 2004) soil properties, and 47.3% higher than when using Nye County soil properties. It is clear in these two figures (Figures 4 and 5), and from comparing average infiltration between soil parameter sets, that using the PTF approach to estimate spatially distributed soil hydraulic properties, in combination with lumping together soil groups 5/7/9, does not lead to underestimates of net infiltration in the next 10,000 years.

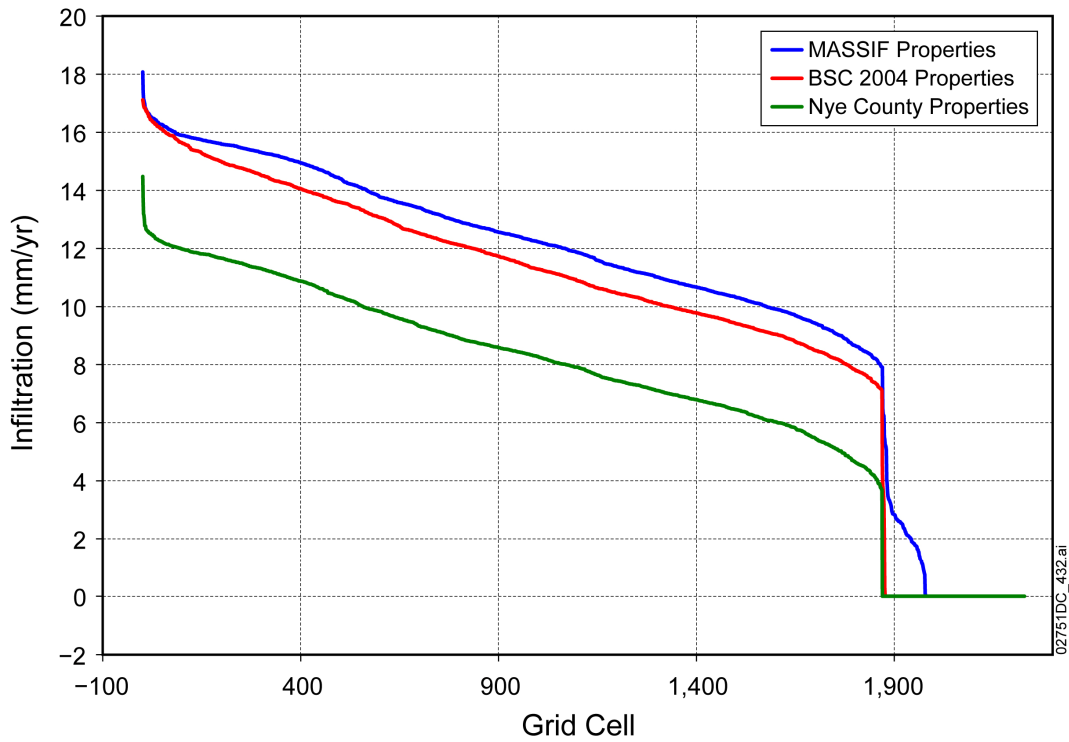


Figure 4. Comparison of MASSIF Model Results for Lower Pagany Wash Using MASSIF, Previous Infiltration Report (BSC 2004), and Nye County Soil Properties

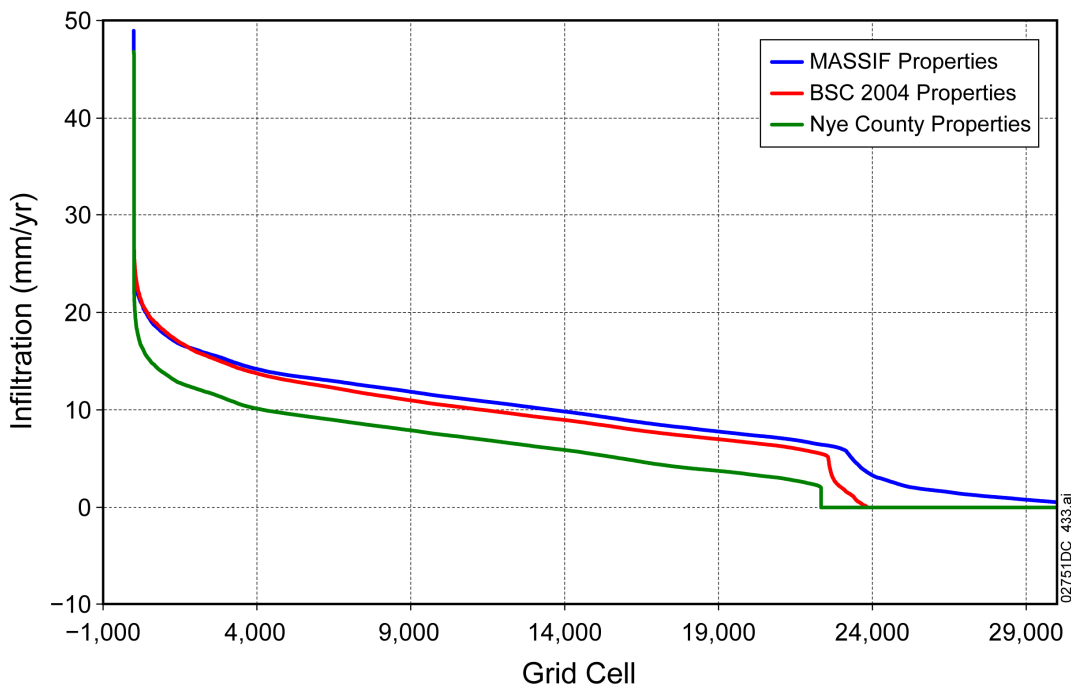


Figure 5. Comparison of MASSIF Model Results for Drill Hole Wash Using MASSIF, Previous Infiltration Report (BSC 2004), and Nye County Soil Properties

## 1.5 SPATIAL VARIABILITY

As discussed in SAR Section 2.3.1.3.3.1.2, characterization of spatial heterogeneities of soil and bedrock properties is accomplished by dividing the model domain into distinct soil groups, soil depth classes, and bedrock type regions inside which the given properties are assumed to be homogeneous. The result of this approach is that the MASSIF model may underestimate the actual spatial variability in net infiltration while characterizing regional infiltration patterns (SNL 2008, Section 6.5.7.6). Thus, the use of a PTF approach, in combination with lumping of soil groups, may result in an underestimation of spatial variability of soil properties. However, the mean annual net infiltration is not underestimated using the PTF and soil lumping approach.

## 1.6 SUMMARY

The soil hydraulic properties used with the MASSIF model as a result of the PTF approach, in combination with lumping of soil groups 5/7/9, do not result in underestimates of net infiltration in the next 10,000 years.

## 2. COMMITMENTS TO NRC

None.

## 3. DESCRIPTION OF PROPOSED LA CHANGE

None.

## 4. REFERENCES

BSC (Bechtel SAIC Company) 2004. *Simulation of Net Infiltration for Present-Day and Potential Future Climates*. MDL-NBS-HS-000023 REV 00. Las Vegas, Nevada: Bechtel SAIC Company. ACC: DOC.20041109.0004.

BSC 2006. *Data Analysis for Infiltration Modeling: Development of Soil Units and Associated Hydraulic Parameter Values*. ANL-NBS-HS-000055 REV 00. Las Vegas, Nevada: Bechtel SAIC Company. ACC: DOC.20060912.0006; DOC.20070102.0003; DOC.20070212.0001.

Guertal, W.R.; Flint, A.L.; Hofmann, L.L.; and Hudson, D.B. 1994. "Characterization of a Desert Soil Sequence at Yucca Mountain, NV." *High Level Radioactive Waste Management, Proceedings of the Fifth Annual International Conference*, Las Vegas, Nevada, May 22-26, 1994. 4, 2755-2763. La Grange Park, Illinois: American Nuclear Society.

Hofmann, L.L.; Guertal, W.R.; and Flint, A.L. 2000. *Development and Testing of Techniques to Obtain Infiltration Data for Unconsolidated Surficial Materials, Yucca Mountain Area, Nye County, Nevada*. Open-File Report 95-154. Denver, Colorado: U.S. Geological Survey.

Istok, J.D.; Blout, D.O.; Barker, L.; Johnejack, K.R.; and Hammermeister, D.P. 1994. "Spatial Variability in Alluvium Properties at a Low-Level Nuclear Waste Site." *Soil Science Society America Journal*, 58, 1040-1051. Madison, Wisconsin: Soil Science Society America.

Khaleel, R. and Freeman, E.J. 1995. *Variability and Scaling of Hydraulic Properties for 200 Area Soils, Hanford Site*. WHC-EP-0883, Rev. 0. Richland, Washington: Westinghouse Hanford Company.

LeCain, G.D.; Lu, N.; and Kurzmack, M. 2002. *Use of Temperature, Pressure, and Water Potential Data to Estimate Infiltration and Monitor Percolation in Pagany Wash Associated with the Winter of 1997–98 El Niño Precipitation, Yucca Mountain, Nevada*. Water Resources Investigations Report 02-4035. Denver, Colorado: U.S. Geological Survey.

ACC: MOL.20020925.0158.<sup>a</sup>

SNL (Sandia National Laboratories) 2008. *Simulation of Net Infiltration for Present-Day and Potential Future Climates*. MDL-NBS-HS-000023 REV 01 AD 01. Las Vegas, Nevada: Sandia National Laboratories. ACC: DOC.20080201.0002; LLR.20080507.0008; LLR.20080522.0101.

USDA (U.S. Department of Agriculture) 2006a. *Primary Characterization Data (Nye, Nevada)*. Lincoln, Nebraska: U.S. Department of Agriculture, Natural Resources Conservation Service. ACC: MOL.20060724.0158.

USDA 2006b. *United States Department of Agriculture (USDA) National Resources Conservation Service Data Reports*. Washington, D.C.: U.S. Department of Agriculture. ACC: MOL.20060710.0217; MOL.20060710.0218; MOL.20060710.0219; MOL.20060710.0220.

NOTE: <sup>a</sup>Provided as an enclosure to letter from Williams to Sulima, dtd 6/5/09, “Yucca Mountain – Request for Additional Information – Volume 3, Chapter 2.2.1.2.1, 5th Set (Scenario Analysis) (Department of Energy’s Safety Analysis Report Section 2.2, Table 2.2-5).”

**RAI Volume 3, Chapter 2.2.1.3.5, First Set, Number 3:**

Clarify whether the presence of faults affects net infiltration within the proposed repository footprint, particularly with respect to focusing from overland and subsurface lateral flow, and if so, how such effects are propagated to the unsaturated zone flow fields (including discretely modeled faults).

This information is needed to evaluate compliance with 10 CFR 63.114(a)(1,2).

Basis: SAR Section 2.3.1 and the supporting infiltration model documentation limit discussion of faults to general description of geomorphology and surficial features associated with faults, but the site-scale unsaturated zone ambient flow model explicitly represents major faults (SAR Section 2.3.2.3.5.4) that intersect 43 proposed emplacement drifts (SAR Table 2.3.4-54). Day et al. (1998) mapped numerous additional faults within the proposed repository footprint that are not explicitly represented in the unsaturated zone ambient flow model. It is not clear if the MASSIF infiltration model accounts for faults and associated differences in rock, soil, and vegetation properties in fault zones (either explicitly or implicitly), and what the technical basis is for the way faults are included in the infiltration model (if they are included) or why they are neglected (if not).

## 1. RESPONSE

Although the Mass Accounting System for Soil and Infiltration (MASSIF) model does not explicitly account for geologic faulting, geologic faulting was included in the detailed characterization of soil textural properties that was used in the model. Such characterization encompassed relevant soil properties that have the potential to affect net infiltration in the model, including faulting. In addition, the MASSIF model used a characterization of soil depth that implicitly captured the effects of faults, and the evaluation of the bedrock saturated hydraulic conductivity took faulting into account.

### 1.1 ESTIMATING HYDRAULIC PROPERTIES FROM SOIL CHARACTERISTICS

The MASSIF infiltration model uses soil hydraulic properties as input in the calculation of net infiltration, in a field-capacity modeling approach, as documented in *Simulation of Net Infiltration for Present-Day and Potential Future Climates* (SNL 2008a). A pedotransfer function (PTF) approach was used to estimate soil hydraulic parameters by matching characteristics of soils collected from the Yucca Mountain site, to those of soils from an analogue site. The approach is described in more detail in the response to RAI 3.2.2.1.3.5-008. Characterization of Yucca Mountain site-specific soil units and associated hydraulic parameters are presented in *Data Analysis for Infiltration Modeling: Development of Soil Units and Associated Hydraulic Parameter Values* (BSC 2006a, Section 6.2.3.1). Soil types were grouped into ten units and are consistent with the United States Department of Agriculture's (USDA) soil classification system (USDA 1999a). The characterization is based on soil samples collected in field studies at Yucca Mountain and vicinity.

Based on the USDA soil classification “triangle” using grain size (USDA 1999b, Exhibit 618-8), grain-size analysis of Yucca Mountain soils indicates that about 68% of the soils are sandy loam, 27% are loamy sand, and 5% are sand. The water holding capacity (WHC) for Soil Group 5/7/9, which combines units 5, 7, and 9 based on their colluvial similarity, is among the most important physical parameters for modeling net infiltration. Colluvial soil type deposits are composed of angular clasts made of rock rubble having finer-grained silt and sand of eolian origin as the support matrix.

## **1.2 EVALUATION OF SOIL DEPTH**

Detailed characterization of spatially varying soil depth at Yucca Mountain has implicitly accounted for the effect of faults associated with depth (BSC 2006b). Faults are associated with the spatial variability of soil depth, particularly in fault-controlled washes with deep soils, and faults that crop out in the caprock or on rock slopes where soils are generally thin. In the MASSIF results, uncertainty in shallow soil depth (i.e., Soil Depth Class 4) has a major effect on net infiltration, whereas uncertainty for deeper soils has a much smaller effect. A summary of sensitivity analyses results are given below.

Soil Depth Class 4 covers most of the repository footprint area, with some area in the northern part covered with Soil Depth Classes 2 and 3 (SAR Figure 2.3.1-19). Soil Depth Classes 2 and 3 have nominal values of soil depth of 16.47 m and 3.26 m, respectively (SNL 2008a, Table 6.5.2.4-3). When compared with topography (SAR Figure 2.3.1-17) and fault locations (Day et al. 1998, Figure 3), the incidence of Soil Depth Classes 2 and 3 in the northern part of the repository footprint corresponds with fault-controlled washes. These include Drill Hole Wash (including Teacup Wash) and Pagany Wash, which covers parts of the repository footprint (also Sever Wash, which is just outside the footprint). The MASSIF uncertainty analyses showed that Soil Depth Classes 2 and 3 have an insignificant effect on net infiltration.

Sensitivity analyses were carried out to identify the parameters that are important to net infiltration in the MASSIF model (SNL 2008a, Sections 6.5.1). The results of the analyses for a fixed precipitation record indicate that the physical parameters most important to net infiltration are the soil depth for Soil Depth Class 4, and WHC for Soil Group 5/7/9. Together, the uncertainties in these parameters account for approximately 90% of the variance in mean net infiltration for the present-day and glacial-transition climates, and about 75% of the variance for monsoon climate. Results of an extended sensitivity analysis showed that the other parameters are responsible for less than 3% of the variance each, and are, therefore, not considered to be as important for estimating mean net infiltration. The sensitivity analyses also showed that net infiltration is mostly insensitive to the saturated hydraulic conductivity of soil and bedrock.

## **1.3 EVALUATION OF BEDROCK SATURATED HYDRAULIC CONDUCTIVITY**

The saturated hydraulic conductivity of the bedrock is calculated as the arithmetic mean of the matrix saturated hydraulic conductivity and the filled-fracture saturated hydraulic conductivity, each weighted by its respective volume fraction. Bedrock fractures associated with older faults tend to be filled. The soil near the surface is subject to continuous exposure to eolian processes, thus contributing to infilling, consistent with the representation of bedrock fractures in the

MASSIF model. Bedrock hydrologic properties were assigned on the basis of lithology, using available information on fracture characteristics for lithostratigraphic units. Although the evaluation of bedrock fractures and calculation of fracture volume fraction for the MASSIF model did not explicitly address the effects of faulting (BSC 2006c, Section 6.5.1), faults were included in the assessment of uncertainty of the volume fraction of fractures. Fracture density generally increases near faults, and data from boreholes located near faults were included in the fracture volume-fraction calculation. Additionally, in the MASSIF model the approach for assessing the upper-bound saturated hydraulic conductivity values, which entailed applying a 200-micron hydraulic aperture to all fractures, accounts for additional unfilled fractures such as may occur near faults (SNL 2008a, Section 6.5.2.6; BSC 2006c, Section 6.5.1).

#### **1.4 EVALUATION OF FAULT CHARACTERISTICS**

Structurally, Yucca Mountain is dominated by subparallel fault blocks that trend to the north and tilt to the east (GI Section 5.2.1). The blocks of ash-flow tuff are bounded by typical Basin and Range style, high-angle, generally west-dipping, normal and oblique faults that formed by rapid east-west extension during the waning phases of Miocene volcanism. Secondary intrablock faults are also common. Studies show that slip rates for active faults in the Yucca Mountain vicinity range from 0.001 to 0.05 mm/yr (SNL 2008b, Section 6.2). Even given uncertainties in slip-rate estimation, these slip rates are classified as low to very low (SNL 2008b, Section 6.2). The slip rates observed at Yucca Mountain fall within the moderately low to low activity fault classification in a regional scheme developed by dePolo (1994, p. 49). Such low fault activity means that the effects of faulting on soil hydraulic properties and soil depth, through disruption of the original surface topography and soil layer, and thus on net infiltration, are minimal. The response to RAI 3.2.2.1.3.5-005 presented a study of focused infiltration in Pagany Wash which is located above a fault zone. The study showed that consequences of more focused infiltration are insignificant to repository performance. Large fluxes in washes are buffered by thick alluvial soil and the presence of the PTn. Such large surface flows resulted in storage rather than seepage below the PTn. Thus, focusing of flow from overland and subsurface lateral flow as a result of faulting in the soil layer is not important to net infiltration. Moreover, the soil near the surface is subject to continuous exposure to eolian and fluvial processes, thereby further minimizing the influence of faulting on net infiltration.

Day et al. (1998) identified the major faults that intersect, or are adjacent to, the repository footprint. Stuckless and Levich (2007) also provided a geological analysis of some of the major faults at Yucca Mountain. SAR Section 2.3.2.2.2 and Figure 2.3.2-10 describe the effect of major faults on flow processes at Yucca Mountain. Of the named faults in the proximity of the repository footprint, all are either (1) block-bounding or outside the footprint (Solitario Canyon, Ghost Dance, Sever Wash), (2) of limited extent (e.g., Sundance), or (3) older (pre-Quaternary; all named faults except the Solitario Canyon). Some of these faults crop out in the cap rock or on rock slopes, over at least part of their intersection with the footprint, which also limits the potential for interception of overland or subsurface flow (Pagany Wash, Sever Wash, and Abandoned Wash). SAR Section 2.3.4 (Table 2.3.4-54) provides data on intersections of known faults with emplacement drifts. The table shows 43 intersections, principally by the Sundance, Drill Hole Wash, Pagany Wash, and West Ghost Dance faults. Comparison of the structural maps (Day et al. 1998, Figures 1 and 3) with maps of designated soil units and soil depth classes

(SAR Figures 2.3.1-18 and 2.3.1-19) confirms the relationships described above. Development of variability and uncertainty distributions for the key parameters of the MASSIF model is consistent with the geological descriptions of the named faults that intersect, or are adjacent to, the repository footprint. SAR Section 2.3.2 (Figure 2.3.2-10) shows major faults represented in the site-scale unsaturated zone flow model domain. As stated in the RAI basis statement above, Day et al. (1998) also mapped additional faults not represented in the unsaturated zone ambient flow model. Such faults are typically small and, therefore, are represented by the MASSIF approach for soil and bedrock properties.

Many developed soils at Yucca Mountain contain cemented carbonate horizons that can impede infiltration. The pedogenic products of desert pavement, petrocalcic accumulations, and argillic horizons tend to fill fractures. These soil characteristics are relevant to fractures potentially caused by faults. Also, carbonate-bearing or petrocalcic soil horizons are reported to have greater water retention capacity than soil types with low carbonate content (Duniway et al. 2004), which further impedes the movement of water. These characteristics are not taken into account in the MASSIF model (BSC 2006a, Section 5.2). Thus, the development of hydraulic properties using the PTF approach tends to conservatively overestimate net infiltration where calcic soils and soil horizons are present (see response to RAI 3.2.2.1.3.5-008 and BSC 2006a, Section 6.4.1).

In summary, faults have minimal effect on the hydraulic properties of the major soil group (Soil Group 5/7/9) and the major soil depth class (Soil Depth Class 4). As stated in Section 1 above, sensitivity analyses showed that the most important physical parameters affecting net infiltration are the soil depth for Soil Depth Class 4, and WHC for Soil Group 5/7/9. It follows that faults have little effect on net infiltration. Considering the geologic description of the faults within or proximal to the repository block, and the representative methodology used to develop the controlling parameters input to the MASSIF model, the effects of faults on focusing of flow from overland and subsurface lateral flow within the soil layer are insignificant. The most important effect of faulting on surface characteristics that are relevant to net infiltration is the effect on soil depth. The variability and uncertainty associated with soil depth are captured in the model.

## **2. COMMITMENTS TO NRC**

None.

## **3. DESCRIPTION OF PROPOSED LA CHANGE**

None.

#### 4. REFERENCES

BSC (Bechtel SAIC Company) 2006a. *Data Analysis for Infiltration Modeling: Development of Soil Units and Associated Hydraulic Parameter Values*. ANL-NBS-HS-000055 REV 00. Las Vegas, Nevada: Bechtel SAIC Company. ACC: DOC.20060912.0006.

BSC 2006b. *Data Analysis for Infiltration Modeling: Technical Evaluation of Previous Soil Depth Estimation Methods and Development of Alternate Parameter Values*. ANL-NBS-HS-000077 REV 01. Las Vegas, Nevada: Bechtel SAIC Company. ACC: DOC.20060918.0009.

BSC 2006c. *Data Analysis for Infiltration Modeling: Bedrock Saturated Hydraulic Conductivity Calculation*. ANL-NBS-HS-000054 REV 00. Las Vegas, Nevada: Bechtel SAIC Company. ACC: DOC.20060710.0001.

Day, W.C.; Dickerson, R.P.; Potter, C.J.; Sweetkind, D.S.; San Juan, C.A.; Drake, R.M., II; and Fridrich, C.J. 1998. *Bedrock Geologic Map of the Yucca Mountain Area, Nye County, Nevada*. Geologic Investigations Series I-2627. Denver, Colorado: U.S. Geological Survey. ACC: MOL.19981014.0301.

dePolo, C.M. 1994. "Estimating Fault Slip Rates in the Great Basin, USA." *Proceedings of the Workshop on Paleoseismology, 18-22 September, 1994, Marshall, California*. Prentice, C.S.; Schwartz, D.P.; and Yeats, R.S., eds. Open-File Report 94-568. Pages 48-49. Menlo Park, California: U.S. Geological Survey.

Duniway, M.C., Herrick, J.E., Monger, H.C., and Brinegar, H. 2004. "The High Water Holding Capacity of Petrocalcic Horizons." *Proceedings, SSSA Annual Meeting*. Las Cruces, NM: USDA. Accessed 02/09/2006. ACC: MOL.20060809.0100.  
URL: <http://web.nmsu.edu/~mduniway/SSSA2004.pdf>.

SNL (Sandia National Laboratories) 2008a. *Simulation of Net Infiltration for Present-Day and Potential Future Climates*. MDL-NBS-HS-000023 REV 01 AD 01. Las Vegas, Nevada: Sandia National Laboratories. ACC: DOC.20080201.0002; LLR.20080507.0008; LLR.20080522.0101.

SNL 2008b. *Features, Events, and Processes for the Total System Performance Assessment: Analyses*. ANL-WIS-MD-000027 REV 00 ACN 01. Las Vegas, Nevada: Sandia National Laboratories. ACC: DOC.20080307.0003; DOC.20080407.0009; LLR.20080522.0166.

Stuckless, J.S. and Levich, R.A., eds. 2007. *The Geology and Climatology of Yucca Mountain and Vicinity, Southern Nevada and California*. Memoir 199. Boulder, Colorado: Geological Society of America.

USDA (U. S. Department of Agriculture) 1999a. *Soil Taxonomy, A Basic System of Soil Classification for Making and Interpreting Soil Surveys*. 2nd Edition. Number 436. Washington, D.C.: U.S. Government Printing Office. ACC: MOL.20060105.0107.

USDA 1999b. "Soil Properties and Qualities." Part 618 of *National Soil Survey Handbook*. Washington, D.C.: U.S. Department of Agriculture.

**RAI Volume 3, Chapter 2.2.1.3.5, First Set, Number 1:**

Describe how net infiltration predicted for Yucca Mountain for the first 10,000 yrs represented in TSPA includes the effect of climate change caused by elevated CO<sub>2</sub> levels related to past and present human activities. This information is needed to evaluate compliance with 10 CFR 63.114(a) (1), (2), (5), and 63.305(a) (b), (c).

Basis: The regulations at 10 CFR 63.305 require that the characteristics of the reference biosphere be consistent with ‘present knowledge’ and DOE must vary factors related to climate consistent with the constraints specified at 10 CFR 63.342(c) (2) for how climate change is to be represented after 10,000 years. For the initial 10,000 years, the influence of elevated greenhouse gases (primarily CO<sub>2</sub>) on climate from past and present human activity is not discussed in SAR Section 2.3.1 on Climate and Infiltration. SNL (2008; Section 6.2, FEPs 1.4.01.00.0A and 1.4.01.02.0A) discusses the distinction between including climate change caused by past and present human activity, and climate change related to potential future changes in human activity. In its screening justification for both FEPs, the applicant maintains that the description of present-day climate is based on “climate records that implicitly include effects of modern society over the duration of historical record.”

NRC staff could not find any other discussion in the SAR or primary AMRs pertaining to how the predicted climate states represented in TSPA reflect trends in global warming related to increased greenhouse gases caused by past and present human activity. The effects of elevated CO<sub>2</sub> and global warming on the climate of Yucca Mountain might not be detected readily in short meteorological records, like those recorded at local and regional meteorological stations.

Of interest are three aspects related to the historical record used to support the climate model in SAR Section 2.3.1.3. One, a discussion or analysis could not be found of the change in climate at YM caused by global warming, and how that change is reflected in the meteorological inputs to the net infiltration model. Two, a discussion could not be found for the duration of the anthropogenic climate changes before the perturbations would be dampened by orbital considerations and any complex feedback mechanisms. Three, how the monsoonal and glacial transition climate analog sites, which were selected based on the paleo-record (e.g., Owens Lake ostracode and diatom record), are appropriate for representing the effect of increased greenhouse gases caused by past and present human activity.

## 1. RESPONSE

Attempting to predict human-induced emissions of greenhouse gases and their potential to effect climate change would involve speculation, and, as a result, introduce inherently large uncertainties in prediction of the future global population behavior and resulting consequences. Consistent with the regulatory framework, anthropogenic effects were not explicitly included in the analysis of future climate. Potential anthropogenic effects, however, are encompassed by the meteorological inputs to the net infiltration model and the future climates states analyzed in the license application.

### 1.1 ANTHROPOGENIC EFFECTS ON METEOROLOGICAL INPUTS TO NET INFILTRATION MODEL AT YUCCA MOUNTAIN

Anthropogenic effects were not explicitly included in the analysis of future climates, but the uncertainty analysis used for the future climate bounds the potential anthropogenic effects. The final environmental impact statement (EIS) (DOE 2002, pp. CR7-108 to CR7-109) acknowledges human-induced climate change and finds that it is within the modeled domain. The final EIS states that DOE considers global warming impacts on future climates to be within the bounds of predicted climate ranges used in the assessment of long-term performance (specifically bounded within the glacial-transition climate state). Uncertainty associated with societal changes, climate, and other long-term phenomena is discussed in the final EIS (DOE 2002, Section 5.2.4.1, p. 5-12), which indicates that conservatism in the climate estimates accounts for these uncertainties.

Human-induced increases in the so-called greenhouse gases (GHG; collectively, carbon dioxide, methane, nitrous oxide, hydrofluorocarbons, perfluorocarbons, and sulfur hexafluoride) have generated much scientific and public discourse because higher levels of atmospheric GHG are believed to act as a trap for outbound long-wave radiation, thus warming the earth. This would likely increase the amount of water vapor in the atmosphere, thus enhancing the hydrologic cycle. Warmth and an energized hydrological cycle would likely lead to greater climate variability from region to region.

Natural levels of CO<sub>2</sub> varied significantly in the past, particularly between glacial and interglacial periods. Low CO<sub>2</sub> levels during glacial periods were succeeded by higher pre-industrial levels over the course of millennia as reflected in some ice cores, and rapid (50 years or less) changes of smaller magnitude occurred during glacial and interglacial periods. The basic individual mechanisms underlying CO<sub>2</sub> variations are known, but the details and dynamics of the overall changes are not. It is not known whether climate changes affected CO<sub>2</sub> levels or vice versa. Changes in the carbon budget, to the extent that they affect climate, already have had and will, in the future, continue to have some effect on the climate of Yucca Mountain (BSC 2004a, p. 6-68).

As stated in excluded features, events, and processes (FEPs) 1.4.01.00.0A (Human Influences on Climate) and 1.4.01.02.0A (Greenhouse Gas Effects), the description of present-day climate, as discussed in included FEP 1.3.01.00.0A (Climate Change), is based on climate records that implicitly include effects of modern society over the duration of the historical record

(SNL 2008a). The infiltration model uses meteorological inputs from the climate analysis that includes temperature, precipitation, and wind speed. The effects of modern society are necessarily implicit rather than explicit in the regional temperature, precipitation, and wind speed data because of the difficulties involved in demonstrating that regional temperature, precipitation, and wind speed signals reflect some measure of recent change beyond natural variability, and in attributing the extent of the change to human activity with some level of confidence. According to the Intergovernmental Panel on Climate Change (IPCC), there has likely been a substantial anthropogenic contribution to global surface temperature increases since the middle of the 20th century; there is less confidence in the understanding of forced changes in other climate parameters, such as surface pressure and precipitation. To the extent that anthropogenic CO<sub>2</sub> contributions have already had an influence on climate, those effects would be in the temperature, precipitation, and wind speed data. It should be noted that the IPCC states that “Difficulties remain in attributing temperature changes at smaller than continental scales and over time scales less than 50 years. Attribution at these scales has, with limited exceptions, not been established” (Hegerl et al. 2007).

The two main factors that control the amount of water that can enter the bedrock as net infiltration are: (1) the amount and frequency of precipitation (and run-on) supplying water to the soil surface, and (2) the extent to which the soil can store the water and allow the processes of evapotranspiration to return water to the atmosphere. Evapotranspiration rates are controlled, in part, by a combination of soil and vegetation properties, and vegetation properties are highly dependent on climate (see SAR Section 2.3.1.3.1.4). Additional climatic variables that affect evapotranspiration rates include air temperature, air humidity, and wind speed (SAR Section 2.3.1.3.3.1.1, pp. 2.3.1-65 to 2.3.1-66).

Climate states selected to represent and bound future climate change in the Yucca Mountain region are referred to as present-day for 0 to 600 years, followed by monsoonal for the next 1,400 years, followed by glacial-transition from 2,000 to 10,000 years after closure. Finally, there is a period from 10,000 to 1,000,000 years for which percolation conditions are defined by regulation, but no explicit climate is defined.

Despite uncertainties in the climate and infiltration analyses, the abstractions of the range in timing of climate change, and the four average annual net infiltration maps representing the 10th, 30th, 50th, and 90th percentile maps for each climate, with associated prior weightings, are sufficient representations for the total system performance assessment (TSPA). This is sufficient because: (1) the range of timing of climate change is small compared to the total length of the glacial-transition period and the post-10,000-year period, and (2) the prior weights of the infiltration maps are adjusted using a quantitative method for assessing the relative agreement between unsaturated zone flow model results and corresponding field observations (SAR Section 2.3.2.4.1.2.4.5.4).

## 1.2 BASIS FOR SELECTING ANALOGUE SITES

SAR Section 2.3.1.2.3.1.2 (p. 2.3.1-27) indicates that the analogue stations provide the upper and lower bounds for precipitation and temperature conditions for each future climate state forecast to occur at Yucca Mountain during the next 10,000 years. This was done because: (1) bounds are needed to quantify uncertainty in input values for the infiltration and TSPA model; and (2) there are uncertainties in the paleoclimate record in regard to extrapolating climate proxy data into climate values. Therefore, establishing possible bounds is more appropriate than establishing mean values, especially for the periods of time under consideration. Because the net infiltration model (SNL 2008b) utilizes annual, seasonal, and daily climate values, the upper-bound and lower-bound values for each climate state were established with meteorological stations selected as representative of the particular climate state. Stations with complete and long records were given priority in the selection process (BSC 2004b, Section 6.6.2). The pooled sites were not intended to represent actual climate states. Rather, as stated in the SAR, the purpose of pooling was to bound uncertainties (SAR Section 2.3.1.2.3.1.2).

Present-day meteorological stations were selected to represent the past climate states defined from the paleo-climate record so that the record of daily temperature and precipitation from these stations can represent future temperature and precipitation (BSC 2004a, Section 6.5.4). Continuous daily temperature and precipitation values from present-day meteorological stations facilitate calculating model-derived future infiltration estimates and those data implicitly include currently observable effects of human-induced climate change for the same reasons stated in Section 1.1. Stations based on geographic location were chosen as analogue climate sites because the shifting of atmospheric circulation patterns over time manifests itself in terms of latitude and longitude. Therefore, present-day meteorological stations positioned with respect to the current seasonal location of the polar front and associated low and high pressure zones were selected as analogues for past climate states.

The geographic areas meeting the requirements for past patterns of atmospheric circulation were selected based on annual and seasonal characteristics of precipitation and temperature (BSC 2004a, Sections 6.1 and 6.5.4). It was necessary to select analogue stations with relatively complete and long records (e.g., 50 years) to encompass temperature, precipitation, wind speed extremes, and events such as the El Niño Southern Oscillation cycle.

The selection of more than one climate station was appropriate to fully characterize climate conditions at a single analogue location. For example, station data from Nogales, Arizona, and Hobbs, New Mexico, were combined to represent the monsoon climate state because monsoon characteristics vary depending on whether the air mass originates in the northern Gulf of California (wet Arizona monsoons) or in the southern Gulf of California or tropical eastern Pacific Ocean (New Mexico monsoons). Including data from both stations incorporates all sources of monsoonal storm tracks that better represent potential future monsoonal storm events at Yucca Mountain.

Using data from one station would not fully represent estimated variability, amount, frequency, and duration of precipitation. The two sites in Arizona and New Mexico were selected because of their temperature and precipitation differences so that a wider range of variability could be

included in infiltration estimates. Likewise, stations in Rosalia, St. John, and Spokane, Washington, although close to each other, do not have identical meteorological records. These stations were selected to collectively represent the upper bound transition climate state to minimize the influence of local meteorological phenomena on the input to the infiltration model (BSC 2004a, Sections 6.5.4 and 6.5.5).

The climate during the monsoonal period would vary from episodes of intense summer rain to present-day-like climates with relatively more winter and less summer precipitation. This description of past monsoon climate is based on paleoecological data from Owens Lake, hydrology, current microfossil species distribution, and precipitation and temperature data, among other paleoenvironmental information (BSC 2004b).

The selected analogue climate stations and the simulated climate in the infiltration model are intended to represent a range of future climate variability for each climate state. A single locality representing an upper or lower bound was purposely not chosen because temperature and precipitation values, seasonality, and extremes in the past cannot be precisely known and it would be inappropriate to base future climate estimates on one modern-day locality. Although not specifically selected to represent potential anthropogenic effects on climate, these analogue sites provide current and past data that constrain future climate states in a manner that bounds the expected (based on literature models) effects of anthropogenic climate changes.

The IPCC reports that annual mean warming in North America is likely to exceed the global mean warming in most areas. Seasonal warming is likely to be largest in summer with maximum summer temperatures likely to increase more than the average in the southwest U.S.A. (Christensen et al. 2007). Annual mean precipitation is likely to decrease in the southwest U.S.A. (Christensen et al. 2007).

The warm, wet monsoon-state climate data included in the infiltration model encompass the estimated increase in temperature that anthropogenic climate change models predict. A 3.5°C average annual warming with slightly greater warming in summer and slightly less warming in winter is projected for the Yucca Mountain region (Christensen et al. 2007, Figure 11.12). Mean annual temperatures at the monsoon climate analogue stations in Nogales, Arizona, and Hobbs, New Mexico, are 17.1°C and 16.6°C, respectively. The mean annual temperature in the Yucca Mountain region is 13.4°C (BSC 2004b, Table 6-29). Therefore, monsoon-state climate data account for the 3.5°C estimated increase in temperature from anthropogenic climate change through 2099. Average minimum/maximum temperatures at Nogales and Hobbs are 5.5/26.1°C and 8.7/24.7°C, respectively (SNL 2006, Tables 7.1-1, 7.1-2, 7.1-3), encompassing the range of temperatures characterizing a monsoon climate state.

Global mean surface temperature increases for the next several thousand years are estimated by Meehl et al. (2007). Global mean surface temperature increases above 3.1°C are very likely. The best estimate with a 650 ppm equivalent CO<sub>2</sub> concentration is a 3.6°C increase, although temperature estimates range from 2.4°C to 5.5°C. If, however, CO<sub>2</sub> equivalent concentration reaches the high level of 1,200 ppm, the best estimate for warming is 6.3°C (Meehl et al. 2007). These estimates assume that the relation between temperature increase and CO<sub>2</sub> holds true for

high CO<sub>2</sub> concentrations and non-linearities in feedback (e.g., clouds, sea ice, and snow cover) are correctly modeled.

A 5% to 10% decrease in average annual and winter (December, January, February) precipitation and a 0% to 5% increase in summer (June, July, August) precipitation is projected for the Yucca Mountain region (Christensen et al. 2007, Figure 11.12). A 5% increase in June, July, and August precipitation based on 32.5 mm total precipitation for these three months at Site 1 (SAR Section 1.1.3.1, Figure 1.1-12) would increase precipitation during this time to 34.1 mm. June, July, and August precipitation for the monsoon climate analogue stations in Nogales, Arizona, and Hobbs, New Mexico, are 211 mm and 163 mm, respectively (WRCC 2008), and annual precipitation values exceed 400 mm/yr (BSC 2004b; SNL 2006, Tables 7.1-1, 7.1-2, 7.1-3). Inputs to the infiltration model are based on these values and thus exceed projected IPCC anthropogenic climate change estimates.

### 1.3 SUMMARY

The effect of long-term responses from anthropogenic activities on the climate in the Yucca Mountain region is not known. Therefore, GHG-forced climate change was not considered directly in selecting future climate analogue stations. In some cases, the kinds of climate change estimated from elevated levels of GHG in literature climate models may share some characteristics of the monsoonal climates that are believed to occur at the ends of the interglacial climates. Some of the future climate models imply a dryer climate. It is conservatively assumed that the present day climate is the driest. Only wetter climates that could cause increased infiltration could have an impact in a negative way on repository performance. However, such negative impacts are bounded by future climate states in the analysis. Therefore, potential anthropogenic changes are encompassed by the climate states used in the analysis.

Present-day precipitation and associated infiltration rates (0 to 600 years) could be impacted if elevated levels of GHG led to a warmer-wetter climate, but this time frame is not significant to performance because the thermal pulse from the repository is projected to be still building, and an increase in infiltration would have no appreciable impact on seepage into the repository. The monsoonal climate state (600 to 2,000 years) could begin earlier as a result of elevated levels of GHG, but again, increased infiltration prior to 600 years would occur while most of the repository area is still above boiling. The glacial-transition climate state (2,000 to 10,000 years after closure) could be pushed further into the future as a result of elevated GHG levels. The glacial-transition climate state would have a colder wetter climate, which would generate higher infiltration rates. In addition, the thermal pulse from the repository would have decayed, allowing for more flux to be converted to seepage within the drifts. Delaying the onset of the glacial transition climate state would likely result in less infiltration, thus enhancing the Upper Natural Barrier capability during that period. The selected analogue climate stations and the simulated climate states in the infiltration model are intended to represent a range of future climate variability for each climate state. Critical factors at a single locality cannot be precisely known and it would be inappropriate to base future climate estimates on one modern-day locality, so multiple localities were chosen to capture the range of variation.

## 2. COMMITMENTS TO NRC

None.

## 3. DESCRIPTION OF PROPOSED LA CHANGE

None.

## 4. REFERENCES

- BSC (Bechtel SAIC Company) 2004a. *Yucca Mountain Site Description*. TDR-CRW-GS-000001 REV 02 ICN 01. Two volumes. Las Vegas, Nevada: Bechtel SAIC Company. ACC: DOC.20040504.0008; LLR.20080423.0019; DOC.20080707.0002.
- BSC 2004b. *Future Climate Analysis*. ANL-NBS-GS-000008 REV 01. Las Vegas, Nevada: Bechtel SAIC Company. ACC: DOC.20040908.0005; DOC.20080813.0003.
- Christensen, J.H.; Hewitson, B.; Busuioc, A.; Chen, A.; Gao, X.; Held, I.; Jones, R.; Kolli, R.K.; Kwon, W.-T.; Laprise, R.; Magaña Rueda, V.; Mearns, L.; Menéndez, C.G.; Räisänen, J.; Rinke, A.; Sarr, A.; and Whetton, P. 2007. "Regional Climate Projections." In *Climate Change 2007: The Physical Science Basis. Contribution of Working Group I to the Fourth Assessment Report of the Intergovernmental Panel on Climate Change*. Eds. Solomon, S.; Qin, D.; Manning, M.; Chen, Z.; Marquis, M.; Averyt, K.B.; Tignor, M.; and Miller, H.L. Cambridge, UK, and New York, NY: Cambridge University Press.
- DOE (U.S. Department of Energy) 2002. *Final Environmental Impact Statement for a Geologic Repository for the Disposal of Spent Nuclear Fuel and High-Level Radioactive Waste at Yucca Mountain, Nye County, Nevada*. DOE/EIS-0250. Washington, D.C.: U.S. Department of Energy, Office of Civilian Radioactive Waste Management. ACC: MOL.20020524.0314; MOL.20020524.0315; MOL.20020524.0316; MOL.20020524.0317; MOL.20020524.0318; MOL.20020524.0319; MOL.20020524.0320.
- Hegerl, G.C.; Zwiers, F.W.; Braconnot, P.; Gillett, N.P.; Luo, Y.; Marengo Orsini, J.A.; Nicholls, N.; Penner, J.E.; and Stott, P.A. 2007. "Understanding and Attributing Climate Change." In *Climate Change 2007: The Physical Science Basis. Contribution of Working Group I to the Fourth Assessment Report of the Intergovernmental Panel on Climate Change*. Eds. Solomon, S.; Qin, D.; Manning, M.; Chen, Z.; Marquis, M.; Averyt, K.B.; Tignor, M.; and Miller, H.L. Cambridge, UK, and New York, NY: Cambridge University Press.
- Meehl, G.A.; Stocker, T.F.; Collins, W.D.; Friedlingstein, P.; Gaye, A.T.; Gregory, J.M.; Kitoh, A.; Knutti, R.; Murphy, J.M.; Noda, A.; Raper, S.C.B.; Watterson, I.G.; Weaver, A.J.; and Zhao, Z.-C. 2007. "Global Climate Projections." In *Climate Change 2007: The Physical Science Basis. Contribution of Working Group I to the Fourth Assessment Report of the Intergovernmental Panel on Climate Change*. Eds. Solomon, S.; Qin, D.; Manning, M.; Chen, Z.; Marquis, M.; Averyt, K.B.; Tignor, M.; and Miller, H.L. Cambridge, UK, and New York, NY: Cambridge University Press.

Sharpe, S. 2003. *Future Climate Analysis—10,000 Years to 1,000,000 Years After Present*. MOD-01-001 REV 01. Reno, Nevada: Desert Research Institute. ACC: MOL.20030407.0055.

SNL (Sandia National Laboratories) 2006. *Data Analysis for Infiltration Modeling: Extracted Weather Station Data Used to Represent Present-Day and Potential Future Climate Conditions in the Vicinity of Yucca Mountain*. ANL-MGR-MD-000015 REV 00. Las Vegas, Nevada: Sandia National Laboratories. ACC: DOC.20070109.0002.

SNL 2008a. *Features, Events, and Processes for the Total System Performance Assessment: Analyses*. ANL-WIS-MD-000027 REV 00. Las Vegas, Nevada: Sandia National Laboratories. ACC: DOC.20080307.0003; DOC.20080407.0009; LLR.20080522.0166; DOC.20080722.0002.

SNL 2008b. *Simulation of Net Infiltration for Present-Day and Potential Future Climates*. MDL-NBS-HS-000023 REV 01 ADD 01. Las Vegas, Nevada: Sandia National Laboratories. ACC: DOC.20080201.0002; LLR.20080507.0008; LLR.20080522.0101.

WRCC 2008, Western Regional Climate Center, Desert Research Institute:  
<http://www.wrcc.dri.edu/>. Accessed 12/26/2008.